University of Denver

Digital Commons @ DU

Electronic Theses and Dissertations   Graduate Studies

1-1-2019

Translation of Partially Decayed Messenger RNAs in Yeast

Ana Luisa Franklin
University of Denver

Translation of Partially Decayed Messenger RNAs in Yeast

Abstract

Flaviviruses are positive-strand single-stranded RNA viruses that are known to form pseudo-knot RNA structures that halt the progression of 5'→3' exonuclease Xrn1. We show that these viral Xrn1-resistant structures (xrRNAs) can be used to protect specific homologously-expressed messenger RNAs from 5'→3' degradation. We investigated the effects of addition of xrRNAs, artificially-installed into the intergenic region of bicistronic mRNA reporters, in the observed levels of protein expression in yeast. The reporters also contain an internal ribosome entry site from the cricket paralysis virus (CrPV IRES) to allow for cap-independent translation of the decay-protected gene, *LacZ*, encoding the enzyme β-galactosidase. Through the use of primer extension, βgalactosidase assay, and western blots, the results indicate that the partially-decayed RNAs are successfully translated, and that addition of xrRNAs results in a 30-50 fold increase in measured enzymatic activity and an accumulation of decay-resistant transcripts in the cell.

Document Type
Thesis

Degree Name
M.S.

Department
Chemistry and Biochemistry

First Advisor
Erich G. Chapman, Ph.D.

Keywords
Decay-resistant, S. cerevisiae, XRN1-resistant, 5'-3' exoribonuclease 1, xrRNAs, Yeast

Subject Categories
Biochemistry | Life Sciences

Publication Statement

Translation of Partially-Decayed

Messenger RNAs in Yeast

_____

A Thesis

Presented to

the Faculty of Natural Sciences and Mathematics

University of Denver

_____

In Partial Fulfillment

of the Requirements for the Degree

Master of Science

_____

By

Ana L. Franklin

June 2019

Advisor: Erich G. Chapman

Author: Ana L. Franklin
Title: Translation of Partially-Decayed Messenger RNAs in Yeast
Advisor: Erich G. Chapman
Degree Date: June 2019

ABSTRACT

Flaviviruses are positive-strand single-stranded RNA viruses that are known to form pseudo-knot RNA structures that halt the progression of 5'→3' exonuclease Xrn1. We show that these viral Xrn1-resistant structures (xrRNAs) can be used to protect specific homologously-expressed messenger RNAs from 5'→3' degradation. We investigated the effects of addition of xrRNAs, artificially-installed into the intergenic region of bicistronic mRNA reporters, in the observed levels of protein expression in yeast. The reporters also contain an internal ribosome entry site from the cricket paralysis virus (CrPV IRES) to allow for cap-independent translation of the decay-protected gene, *LacZ,* encoding the enzyme β-galactosidase. Through the use of primer extension, β-galactosidase assay, and western blots, the results indicate that the partially-decayed RNAs are successfully translated, and that addition of xrRNAs results in a 30-50 fold increase in measured enzymatic activity and an accumulation of decay-resistant transcripts in the cell.

TABLE OF CONTENTS

LIST OF FIGURES

LIST OF ABBREVIATIONS

Abbreviation	Meaning
ATP	Adenosine triphosphate
ATPase	Adenosine triphosphatase
BP	Base pair
CBC	Cap-binding complex
cDNA	Complementary DNA
CPSF	Cleavage and polyadenylation specificity factor
CrPV	Cricket paralysis virus
CStF	Cleavage stimulation factor
CTD	Carbon-terminal domain
DNA	Deoxyribonucleic acid
DSE	Downstream sequence element
DXO1	Decapping exonuclease 1
EDTA	Ethylenediaminetetraacetic acid
eEF-1α	Eukaryotic elongation factor 1α
eEF-2	Eukaryotic elongation factor 2
eIF1	Eukaryotic initiator factor 1
eIF1A	Eukaryotic initiator factor 1A
eIF2	Eukaryotic initiator factor 2
eIF3	Eukaryotic initiator factor 3
eIF4A	Eukaryotic initiator factor 4A
eIF4F	Eukaryotic initiator factor 4F
eIF4F	Eukaryotic initiator factor 4F
eIF4G	Eukaryotic initiator factor 4G
eIF5	Eukaryotic initiator factor 5
eRF1	Eukaryotic release factor 1
eRF3	Eukaryotic release factor 3
GAPDH	Glyceraldehyde 3-phosphate dehydrogenase

Abbreviation	Meaning
GDP	Guanosine diphosphate
GTFs	General transcription factors
GTP	Guanosine triphosphate
GTPase	Guanosine triphosphatase
HCV	Hepatitis C virus
IRES	Internal ribosome entry site
m^7G	5' 7-methylguanylate cap
MBG H_2O	Molecular Biology Grade water
Met-tRNA$_i^{Met}$	Initiator tRNA-methionine
mRNA	Messenger RNA
mRNPs	Messenger ribonucleoproteins
ODCase	Orotidine 5'-phosphate decarboxylase
ORF	Open-reading frame
PABP	Poly(A)-binding protein
PIC	43S preinitiation complex
RCF	Relative centrifugal force
RNA	Ribonucleic acid
RNAPII	RNA polymerase II
SD media	Synthetic defined media
sfRNAs	Subgenomic flavivirus RNAs
TBP	TATA-binding protein
TFIIA	Transcription factor II A
TFIIB	Transcription factor II B
TFIID	Transcription factor II D
TFIIE	Transcription factor II E
TFIIH	Transcription factor II H
tRNA	Transfer RNA
UTRs	Untranslated regions
WT	Wild-type
XRN1	5'-3' exoribonuclease 1
xrRNAs	Xrn1-resistant RNAs
YPAD	Yeast peptone plus adenine media
YPD	Yeast peptone dextrose media

CHAPTER ONE: INTRODUCTION

1.1   <u>Eukaryotic mRNA</u>

The central dogma of molecular biology paints a simple picture of the flow of genetic information in the cell: DNA is used as a blueprint to make messenger RNA (mRNA), which in turn gets translated into protein. In reality, the transfer of genetic information follows a dynamic system in which the flow of information is heavily regulated in a bilateral fashion (Vihervaara et al., 2008). Cells have evolved complex and precise regulatory systems to alter the rate of gene expression in response to internal or external stimuli with the use of enzymes and regulatory molecules. An important aspect of gene expression is the regulation of mRNA levels in the cell, which is highly dependent on the rate of two opposing processes: transcription and decay (Alonso, 2012).

Decay of mRNA transcripts can occur via different redundant pathways in yeast (Parker, 2012). In the 5'$\rightarrow$3' direction, the major exonuclease responsible for mRNA decay is the enzyme XRN1, which recognizes a 5' monophosphate left behind after the 5' cap is removed by a decapping enzyme (Geerlings et al., 2000). Viral pseudoknot RNA

structures known as xrRNAs have been shown to resist decay by XRN1 by presenting the enzyme with a mechanical barrier. These XRN1-resistant structures are known to protect fragments of the viral genome from degradation, resulting in the accumulation of decay-resistant fragments that have been linked to increased pathogenicity in the infected cells (Chapman et al., 2014a, 2014b, Akiyama et al., 2016). By studying these decay-resistant structures, it may be possible to gain insight on gene expression regulatory mechanisms, as well as possibly discovering ways of combatting and/or attenuating certain kinds of viral infections. xrRNAs can potentially be used in molecular biology to protect desired mRNAs from degradation, which should result in increased protein synthesis after the genes encoded within those decay-resistant mRNA fragments are translated. This work concentrates on investigating the effects of addition of xrRNAs to previously-characterized yeast reporters by qualitative and quantitative analysis of the protein and mRNA content of the resulting cells.

1.1.1 Transcription

The lifecycle of an mRNA molecule begins with transcription. By definition, transcription is the formation of an RNA molecule from a DNA template and requires the use of a DNA-dependent RNA polymerase. In eukaryotes, the main enzyme responsible for mRNA transcription in the nucleus is RNA polymerase II (RNAP II). Transcription begins when RNAP II is recruited to the promoter region of a protein-coding gene with the help of several general transcription factors (GTFs). A promoter region is a sequence element in the DNA that is recognized by specific transcription factors as a binding site,

triggering a cascade of events that lead to transcription initiation. Promoters can be constitutively active (e.g. house-keeping genes), or inducible, in which genes are turned on or off in response to changes in cellular conditions. An example of an inducible promoter is the galactose promoter that regulates the transcription of genes required for galactose catabolism, which ensures that the genes are transcribed if (and only if) they are required for cell growth and survival (Douglas and Condie, 1954; Douglas and Hawthorne, 1964). Since glucose is a repressor of the galactose promoter, and galactose is an activator, the genes are only transcribed in the absence of glucose and presence of galactose. Otherwise, the cells rely on glucose catabolism, which provides more ATP per molecule and is thus the favorable catabolite. The use of a galactose-inducible promoter in cellular biology allows for a higher control of experimental conditions, since the genes can easily be turned on or off as needed by simply switching the growth media.

Five GTFs have been shown to be essential for transcription and are highly conserved in all eukaryotes: TFIID, TFIIB, TFIIF, TFIIH, and TFIIE (Orphanides et al, 2019). For RNAP II-mediated transcription, a subunit of TFIID (TBP, or TATA-Binding-Protein) recognizes and binds to the TATA element present in a great variety of promoters. TFIIB then recognizes the TFIID-promoter complex and binds, followed by binding of TFIIE, TFIIH and TFIIA to complete the preinitiation complex. The DNA strands are separated around the promoter region (promoter melting), providing the single-stranded template necessary for RNAP II to begin mRNA synthesis. Transcription begins with extensive phosphorylation of the carbon-terminal domain (CTD) of RNAP II by TFIIH, and formation of the first phosphodiester bond between two RNA bases.

1.1.2   Processing and Transport

Processing of the RNA transcript into a mature mRNA occurs cotranscriptionally with three major reactions: capping, splicing, and polyadenylation. This process begins when the emerging RNA transcript is about 20-30 nucleotides long by the addition of a 5' cap. This occurs in three steps: 1) the triphosphate of the first RNA nucleotide is hydrolyzed by RNA triphosphatase, resulting in a bisphosphate group, 2) A GMP is added to the bisphosphate via a 5'-5' linkage by a guanyltransferase, and 3) The N7 position in the added GMP is methylated by a methyltransferase, resulting in the 5' 7-methylguanylate cap (m^7G) (Proudfoot et al, 2002). The unusual 5'-5' linkage of the m^7G cap provides stability to the RNA molecule (Beelman and Parker, 1995) and is recognized by the cap-binding complex (CBC), which remains bound to the mRNA until it has been exported to the cytoplasm.

In general, eukaryotic genes are made up of coding regions (exons) interrupted by noncoding regions (introns). Splicing is the removal of introns and merging of exons into a single open-reading frame that can be subsequently translated into protein. Splicing occurs via two reactions (each followed by transesterification): 1) Nucleophilic attack of the 2'OH on the branchpoint adenosine onto the 5' end of exon 1, resulting in a lariat intermediate and a free exon 1, and 2) Nucleophilic attack of 2'OH of exon 1 ono the 5' end of exon 2, resulting in the spliced pre-mRNA and free intron (More and Sharp, 1993). These reactions are facilitated by the spliceosome, made up of small nuclear RNAs (U1, U2, U4, U5, and U6) and their associated proteins (For review, see Kramer, 1996).

Most mRNAs contain a 3' end made up of about 250 adenosine residues, known as the poly(A) tail. Before the poly(A) tail is added, the pre-mRNA is cleaved downstream from the polyadenylation signal, which is a highly conserved hexamer of sequence AAUAAA, followed by a downstream sequence element (DSE) composed of a U- or GU-rich motif. Cleavage and polyadenylation specificity factor (CPSF) binds directly to the hexameric polyadenylation signal and is the main enzyme responsible for cleavage of the pre-mRNA approximately 10-30 nucleotides downstream from its binding site (usually between the hexamer and DSE). Cleavage usually occurs before transcription termination, and cleavage stimulation factor (CStF) binds to both the RNA and RNAP II, signaling it to release the transcript (Glover-Cutter, 2008). Once the pre-mRNA has been cleaved, the enzyme polyadenylate polymerase (poly(A) polymerase) catalyzes the addition of single adenosine monophosphate units to the 3' end, until the tail is approximately 250 nucleotides long (For review, see Wahle and Ruegsegger, 1999).

Once capped, spliced, and polyadenylated, mature mRNAs can be transported from the nucleus to the cytoplasm. Mature mRNAs remain bound to several proteins, forming mature messenger ribonucleoproteins (mRNPs). The associated proteins serve to stabilize the RNA, and direct it to the cytoplasm. Among these proteins, the CBC plays a crucial role in transport through the nuclear pore complex, along with the DEAD box protein, Dbp5 (Hamm, 1990; Rocak and Linder, 2004). Once in the cytoplasm, the translation process can begin.

1.1.3 <u>Translation</u>

A mature mRNP consists of at least one protein-coding gene, also called open

reading frame (ORF), flanked by 3' and 5' untranslated regions (UTRs), protected by a 5'

cap and 3' poly(A) tail, and complexed with several proteins. The translation of mRNAs

primarily occurs by a 5' cap-dependent pathway: initiation of translation involves the

interaction of the ribosome, among other key proteins, with the 5' cap and 5' UTR of the

mRNA. Proteins importin-α and importin-β are responsible for exchanging the CBC with

the cap-binding protein eIF4F (eukaryotic Initiator Factor 4F), which mediates the

initiation of the standard cap-dependent translation (Sato and Maquat, 2009;

Gonatopoulos-Pournatzis and Cowling, 2013).

Eukaryotic ribosomes (80S) are composed of two subunits: the small subunit

(40S) and the large subunit (60S). The first step in translation initiation involves the

binding of the initiator tRNA (Met-tRNA$_i^{Met}$) to the P site of the small ribosomal subunit.

This is achieved with the help of eIF2, which complexes with the tRNA, the 40S subunit

and GTP, which is required for translation initiation (Sonenberg and Dever, 2003). The

resulting eIF2•GTP•Met–tRNA$_i^{Met}$ ternary complex (FIGURE 1), joined by the 40S

subunit, eIF1, eIF1A, eIF3 and eIF5 form the 43S preinitiation complex (PIC) (Algire *et*

al., 2002). The PIC is recruited by eIF4F. eIF4F consists of three subunits: eIF4A, eIF4E

and eIF4G. eIF4E is responsible for binding to the 5' cap, while eIF4A serves as an

ATPase and ATP-dependent RNA helicase (Sonenberg, 1996). eIF4G is a scaffold

protein that also binds eIF3, which associates with the 40S ribosomal subunit (Pain,

1996). The poly(A)-binding protein (PABP) binds to the poly(A) tail, which has been

6

shown to be essential for effective translation initiation (Jacobson, 1996; Sachs et al,

1997). In yeast, PABP has been shown to associate with eIF4G (Tarun and Sachs, 1996).

In poly(A) tail-dependent translation, the mRNA circularizes following the closed loop

model, in which the 3' end of the mRNA loops around to the 5' end (Kahvejian, 2001;

Tarun and Sachs, 1996).
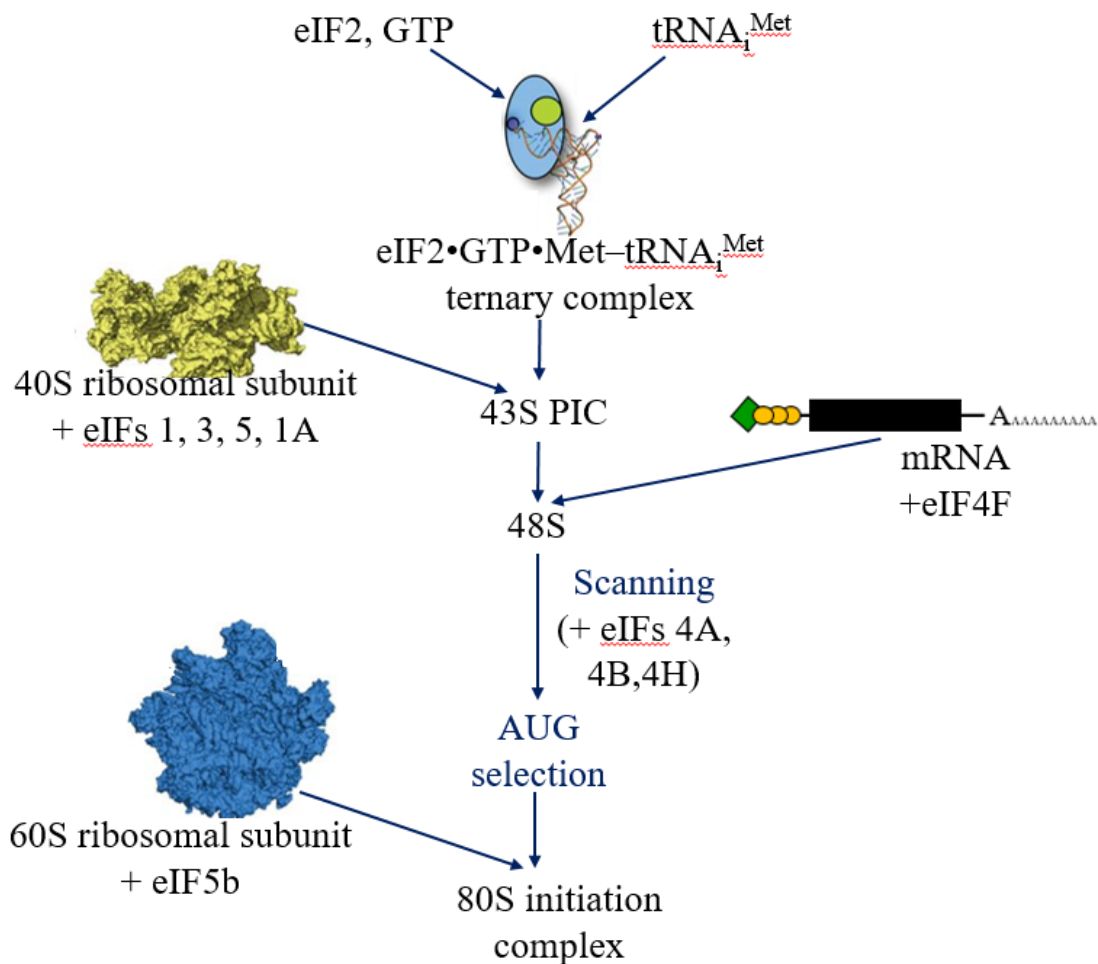
FIGURE 1. Assembly of the eukaryotic 80S ribosome capable of translation initiation. The eIF2•GTP•Met–tRNA$_i^{Met}$ ternary complex is vital for proper formation of the cap-dependent translation initiation complex (Figure adapted from Pavitt & Proud, 2009).

Once formed, the PIC is recruited to the 5' cap of the mRNA and, once bound, scans the 5' UTR of the mRNA in the 5'→3' direction until it locates the start codon, AUG (Hinnebusch, 2011). Once the start codon is reached, the PIC releases eIF1, which triggers a change in conformation of the complex and GTP hydrolysis, releasing an inorganic phosphate. eIF5, the GTPase responsible for this hydrolysis reaction, and eIF2•GDP are subsequently released (Maag et al, 2005). The eukaryotic initiation factors 1A and 5B (a second GTPase) mediate the assembly of the 60S ribosomal subunit, forming the 80S initiation complex. Binding of the 60S subunit triggers GTP hydrolysis by eIF5B, which leads to conformational changes in the complex, resulting in release of eIF5B (Pestova et al, 2000). Finally, eIF1A is released (Acker et al, 2009), resulting in a fully-assembled 80S ribosome capable of protein synthesis (For comprehensive review of translation initiation, see Aitken and Lorsch, 2012).

Elongation begins with the initiator tRNA bound to the P (peptidyl-tRNA) site of the 80S ribosome. The eukaryotic elongation factor 1α (eEF-1α), which binds to GTP and the aminoacyl-tRNA, directs the binding of the corresponding amino acid to the next codon in the mRNA sequence, located at the A site. When the correct match has been made, GTP is hydrolyzed, eEF-1α •GDP is released, and the aminoacyl-tRNA is placed at the A site. The peptidyl transferase center located in the 60S subunit can then catalyze peptide bond formation between the two amino acids in the P and A sites. The initiator methionine is released from the P site, transferring the nascent polypeptide onto the A site. The mRNA is shifted down one codon, leaving the deaminoacylated initiator tRNA at the E (exit) site, and the tRNA containing the polypeptide chain at the P site. The

translocation step is mediated by eEF-2, and also requires GTP hydrolysis. The initiator tRNA exits and a new aminoacyl-tRNA enters at the A site. This cycle is repeated for the rest of the coding region of the mRNA (Merrick, 1992), until one of three stop codons is reached (UAA, UGA, or UAG). Termination of translation begins when the stop codon is recognized by eukaryotic release factor 1 (eRF1). After eRF3 hydrolyzes GTP, eRF1 releases the polypeptide from the tRNA located in the P site (Hellen, 2018). The post-termination complex is subsequently disassembled, freeing all the components and allowing them to enter another cycle of translation.

1.1.3.1 Eukaryotic Versus Prokaryotic Translation

There are important distinctions between eukaryotic and prokaryotic mRNAs. As explained above, in eukaryotes, the processes of transcription and translation are separated in space and time. Prokaryotic cells, on the other hand, do not contain a nucleus and therefore do not require transport of mRNAs to the cytoplasm. In prokaryotes, the processes of transcription and translation do not only occur in the same place, but also can occur simultaneously. Prokaryotic translation can begin before the process of transcription is complete, with ribosomes having the capability of binding to nascent mRNAs. In comparison to eukaryotic mRNAs, prokaryotic mRNAs require almost no post-transcriptional modifications and have a significantly lower lifetime.

1.1.3.2 <u>Internal Ribosome Entry Sites (IRES)</u>

Another important distinction is the number of genes encoded in each mRNA. Eukaryotic mRNAs are typically monocistronic, indicating that each mRNA contains a single ORF, encoding for a single polypeptide. In contrast, prokaryotic mRNAs can contain multiple ORFs. Only the first ORF in a polycistronic mRNA can be translated via cap-dependent translation, since the ribosome-mRNA interaction is broken once the ribosome reaches the stop codons present at the 3' end of the first ORF. An internal ribosome entry site (IRES) is a cis-acting RNA element that, when present upstream from a coding region, can be recognized by and act as a binding site to a ribosome, thus allowing for cap-independent translation. IRES structures were first discovered in picornaviral mRNAs (Jang et al., 1988; Pelletier and Sonenberg, 1988), and were originally believed to function exclusively in prokaryotes (Kozak, 1979; Kanarska et al., 1981), since eukaryotic ribosomes were reportedly unable to bind circular mRNAs. The picornaviral IRES was found to be a 450-nucleotide structure located at the 5'UTR of the viral genome (Jackson et al., 1990). Initiation of translation via an IRES differs from the canonical mechanism, since the ribosome binds directly to the entry site, rather than scanning for the start codon after binding to the 5' end. The notion that IRES structures could only function in prokaryotes was disproven when it was shown that insertion of this structure into the intron of bicistronic eukaryotic mRNAs could mediate translation initiation via internal entry of the ribosomes (Jang et al., 1988; Pelletier and Sonenberg, 1988). Up to date, a large number of non-prokaryotic IRES structures have been found,

both in viral and eukaryotic mRNAs encoding for a wide range of proteins (For review, see Hellen and Sarnow, 2019).

1.1.3.2.1   Mechanisms of Internal Ribosomal Entry

Current knowledge suggests that there is no universal IRES structure or mechanism of internal ribosomal entry. No important parallels have been made in respect to size, sequence, or structure between all known IRES elements. So far, three mechanisms of translation initiation via internal ribosomal entry have been differentiated. The first mechanism is observed in members of the *Picornaviridae* family. Although IRES elements have been discovered for all known members of this viral family, there are at least three distinct structural motifs observed, with members of each genus displaying similar characteristics (Brown et al., 1991; Borman and Jackson, 1992; Hinton and Crabb, 2001; Bakhshesh et al., 2008). Despite their structural features, all IRES elements of the *Picornaviridae* family recruit the ribosome with the help of translation initiation factors and RNA binding proteins, including eIF4G, the poly(A) binding protein (PABP) and the eIF3/eIF2•GTP•Met–tRNA$_i^{Met}$ ternary complex. In short, eIF4G and PABP interact around the IRES elements, leading to a pseudo-circularization of the mRNA that is similar to that observed in cap-dependent translation (Martinez-Salas et al., 2015). In contrast to the factor-dependent mechanism observed in the *Picornaviridae* family, the IRES from hepatitis C virus (HCV) is able to bind the 40S ribosomal subunit in the absence of any initiator factor. The HCV IRES is a 410-nucleotide-long stem-loop secondary structure that consist of most of the viral 5' UTR and interacts directly with the

40S subunit, which in turn binds to eIF3. The start codon has been shown to be located on loop IV of the structure, right on (or very near) the P-site of the bound ribosomal subunit (Pestova et al., 1998).

1.1.3.2.2   Translation Initiation without Initiator tRNA (The CrPV IRES)

The third method of internal ribosomal entry, discovered in the cricket paralysis virus (CrPV), is not only independent of initiator factors in order to achieve IRES•40S subunit complex formation, but also does not require eIF2, an initiator tRNA, or GTP hydrolysis in order to achieve the fully-functional IRES•80S ribosome complex (Hellen and Sarnow, 2019). The CrPV IRES has been shown to bind the 40S ribosomal subunit, then recruit the 60S subunit directly, initiating translation from the A site (rather than the P site) of the ribosome (Wilson et al., 2000). Internal translation initiation by the CrPV IRES also differs from the canonical mechanism in that the first amino acid in the resulting polypeptide is not methionine, but either alanine or glutamine (Sasaki and Nakashima, 1999).

The CrPV IRES is 192 nucleotides long, commonly forming an extensive triple-nested pseudoknot (Kanamori and Natashima, 2001; Thompson and Gulyas, 2001; Schüler et al., 2007). It contains a smaller pseudoknot structure (42 nucleotides long) at the 3' end that has been shown to be essential for translation initiation, since internal translation initiation has been disrupted in mutants that exhibit improper pseudoknot formation (FIGURE 2) (Sasaki and Nakashima, 1999; Domier et al., 2000, Wilson et al, 2000). The pseudoknot is immediately followed by the coding triplet, which is either

12
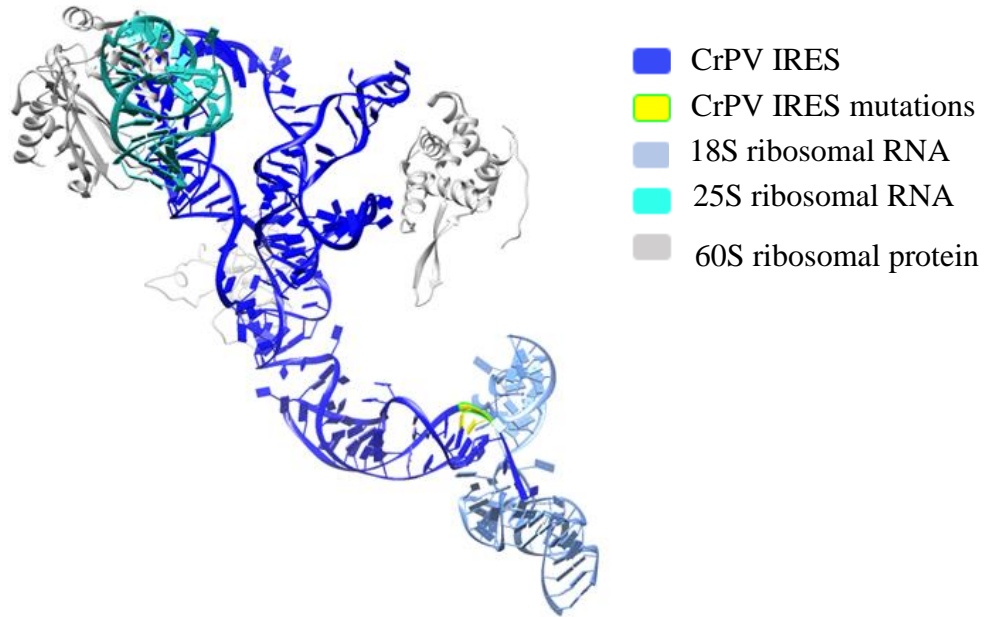
FIGURE 2. Stereo view of ribosome-bound CrPV IRES structure (PDB 2NOQ, adapted from Schuler et al., 2007). Mutations that prevent formation of the small 3'end pseudoknot formation and inhibit internal ribosomal initiation are highlighted in yellow.

GCU or GCA in all CrPV-like IRESs that have been studied. Helical regions of the CrPV-like IRES elements are believed to play a key structural role, since there is high sequence specificity in these regions (Hellen and Sarnow, 2019). The mechanism through which the CrPV IRES recruits the ribosome is believed to be an unprecedented stance of tRNA- and mRNA-mimicking, since recent cryo-microscopy structures of an IRES•Ribosome•aminoacyl-tRNA complex show a conformation in which the IRES binds to the E site of the ribosome mimicking the acceptor stem of a tRNA (Pisareva et al., 2018). The structures shows a doubly-translocated IRES structure with the aminoacyl-tRNA occupying the P site. This suggests that the IRES is not only able to trigger translation initiation without the need for the initiator tRNA, but that it is also able to translocate twice (lacking prior peptide-bond formation), leaving the ribosome ready

for elongation. Thus, the IRES element can mimic mRNA in order to recruit the 40S subunit of the ribosome, and mimic tRNA in order to initiate protein synthesis. This double-mimicking mechanism allows the CrPV IRES to bind the ribosome and prime it for translation elongation, without the need for eukaryotic initiation factors.

1.1.4   mRNA Half-Lives and Stability

Once an mRNA molecule has been transcribed, it has a specific lifetime after which it is broken down into individual bases, which can be subsequently recycled into new mRNAs. Mammalian mRNAs have been found to have half-lives ranging from a few minutes to over 24 hours (Sharova et al., 2009). Even mRNAs with very short half-lives can be translated more than once. Once an 80S ribosome has assembled at the 5' end of the mRNA and translation has initiated, the ribosome will travel in the 5'$\rightarrow$3' direction along the mRNA, decoding every codon and adding the corresponding amino acid to the growing peptide chain, until it reaches a stop codon. This frees up the 5' end, enabling a second ribosome to assemble, and so on, resulting in several ribosomes loaded onto a single mRNA. Furthermore, following the closed-loop model, once the ribosome reaches the stop codon at the 3' end of the mRNA, the 5' end is in close proximity, allowing for the newly released ribosome to bind again and begin a new round of translation. In human cells, the protein-to-mRNA ratio has been found to vary greatly, ranging from 1×10^2 to 1×10^8, with most ratios ranging over more than two orders of magnitude (Eraslan et al., 2019).

An important factor affecting mRNA lifetime is its stability, which in turn can be determined by its sequence and structure (Ross, 1995). Primary and secondary structure of an mRNA are cis-determinants of its stability. These cis-determinants include the poly(A) tail, 5' and 3' UTRs, and the mRNA coding region. In general, these cis-enhancers of stability are sequences that can basepair to form a more stable secondary structure; even the smallest changes in secondary structure have been found to have the ability to influence mRNA half-lives (Weiss and Liebhaber, 1994). There are many other factors that determine the stability of an mRNA, including its translation rate, cellular location and environment, as well as the presence of regulatory factors. Trans-acting factors include RNA-binding proteins that shield mRNAs from degradation, including PAPB (Ross, 1995).
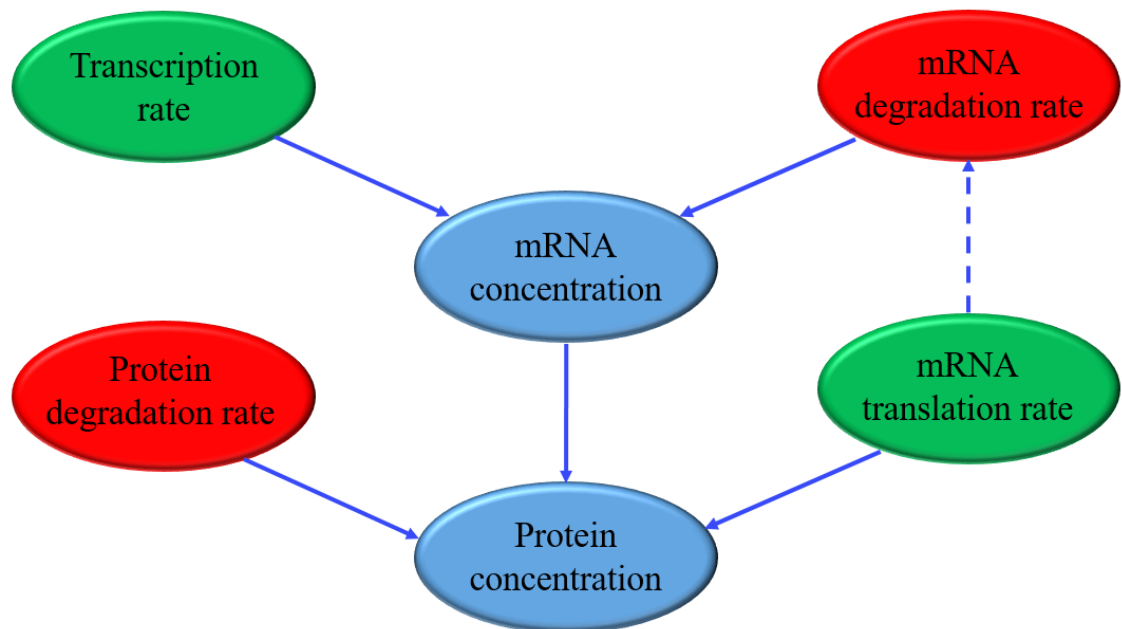
FIGURE 3. The concentration of mRNAs in the cell is highly dependent on the rates of two opposing processes: transcription and mRNA decay. Similarly, the major factors affecting protein concentrations are: mRNA abundance, and rates of translation and protein degradation.

15

1.1.5   mRNA Turnover

After an mRNA has fulfilled its biological role, it must be degraded in order to

prevent buildup of products and intermediates in the cell (FIGURE 3). As previously

discussed, eukaryotic mRNAs are stabilized by interactions of the 5' cap and the poly(A)

tail with eIF4G and PAPB. The poly(A) tail is progressively shortened over time

(Sheiness and Dernell, 1973). The process of mRNA degradation begins once the length

of the poly(A) tail is approximately 10 nucleotides long, making the oligo(A) tail too

short to maintain a physical interaction with PAPB (Decker and Parker, 1993; Muhlrad

and Parker, 1992; Muhlrad et al., 1994). After this, the mRNA is degraded by one of two

redundant pathways: the exosome-mediated 3'$\rightarrow$5' pathway, or in the decapping-

dependent 5'$\rightarrow$3' pathway. In the 3'$\rightarrow$5' pathway, the unprotected 3' end is attacked by

the exosome, which is a large complex of 3'$\rightarrow$5' exoribonucleases (Mitchell and

Tollervey, 2003; Garneau et al., 2007).

In the 5'$\rightarrow$3' decay pathway, the shortening of the poly(A) tail, which is thought

to in turn destabilize the cap-binding complex, is followed by decapping. The main

enzyme responsible for decapping in yeast is Dcp1p, which is believed to recognize the

mRNA substrate by interacting with both the 7-methyl group on the cap structure and the

RNA portion of the mRNA (LaGrandeur and Parker, 1998; Caponigro and Parker, 1996).

Removal of the m^7G cap exposes a 5' monophosphate which is the substrate for the

enzyme Xrn1 (Hsu and Stevens, 1993; Muhlrad et al., 1994). The exonucleolytic activity

of Xrn1 continues in the 5'$\rightarrow$3' direction, removing one nucleotide at a time and

exposing a new 5' monophosphate each time, until the entire mRNA is degraded

(FIGURE 4).
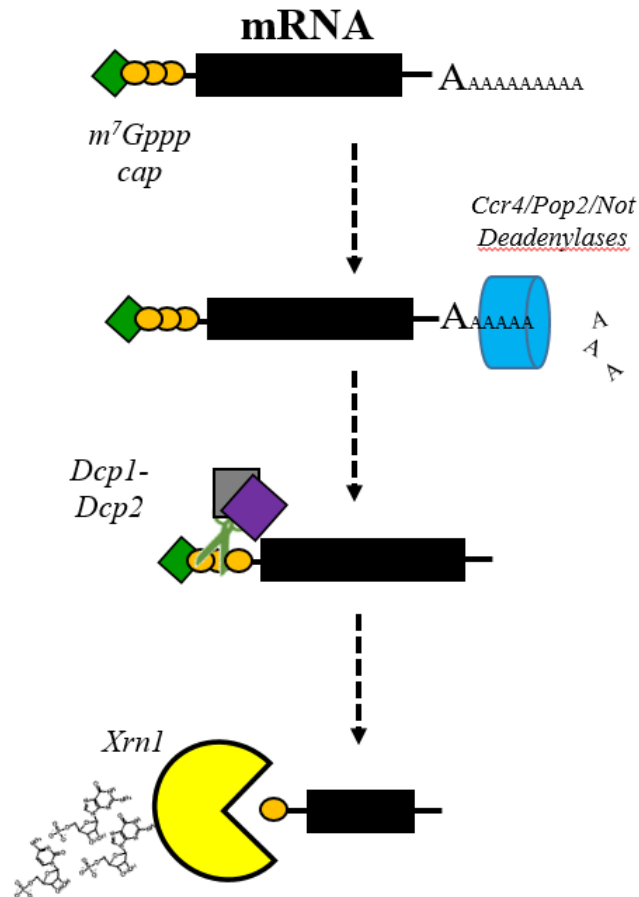
FIGURE 4. Overview of 5'→3' mRNA decay pathway. The mRNA is committed to decay after progressive deadenylation of the poly(A) tail results in a short oligo(A) tail. Degradation continues by removal of the m^7G cap by a decapping enzyme, which exposes a 5' monophosphate that is the substrate for the exoribonuclease, XRN1. XRN1 is the major 5'→3' exoribonuclease and completely degrades the remainder of the mRNA sequence by cleaving off one nucleotide at a time.

1.2   Partially-Decayed RNAs

1.2.1   *Flaviviridae* and Sub-Genomic RNAs

Flaviviruses are pathogenic plus-sense single-stranded RNA viruses that include the West Nile virus, Zika virus, and yellow fever virus (Westaway, 1985). Upon infection, flaviviruses utilize the host's cellular enzymes in order to replicate their genomic RNA. In addition, this process also generates noncoding RNA's called subgenomic flavivirus RNAs (sfRNAs) that are linked to increased pathogenicity (Pijlman et al., 2008; Liu et al., 2014). These sfRNAs are now known to be the result of incomplete decay by the exonuclease Xrn1 (Jones et al., 2012). This is due to the formation of pseudo-knot structures found in the 3' untranslated region of the viral genome (3'UTR), which halt the progression of Xrn1 in the 5'$\rightarrow$3 direction (Chapman et al., 2014a, 2014b, Akiyama et al., 2016), protecting any downstream genetic material from degradation in that direction. The pseudoknot is composed of a three-helix junction, through which the 5' end is threaded, thus providing a mechanical barrier against Xrn1's exonucleolytic activity (FIGURE 5). These Xrn1-resistant structures (xrRNAs) can potentially be used to target certain genes from degradation and are expected to increase protein synthesis of such genes.

1.3   *S. cerevisiae* as a Model Organism

Yeast are unicellular eukaryotes that can reproduce either by sexual or asexual reproduction. Being one of the simplest eukaryotic organisms, yeast make popular model organisms for laboratory studies. The baker's or budding yeast, *Saccharomyces*

18

cerevisiae, is one such model organism. The S. *cerevisiae* genome was the first

eukaryotic genome to be fully sequenced (Goffeau et al., 1996) and is very well

characterized. S. *cerevisiae* cells are easy to grow and maintain, due to their short

generation time and flexibility to adjust to changing environmental conditions.

Furthermore, their genome is easily manipulated and a full collection of ORF knockouts

exists (Shoemaker et al., 1996; Chu and Davis, 2008), making S. *cerevisiae* an ideal

candidate for molecular biology studies.
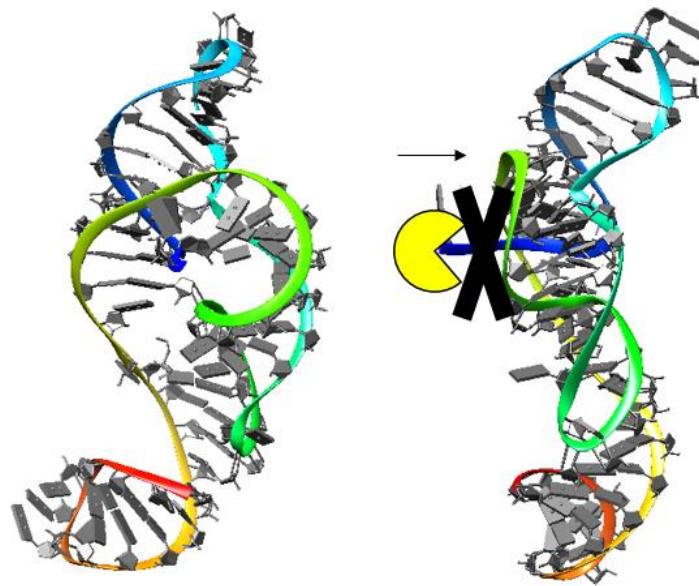
FIGURE 5. ZIKV xrRNA front and side views. 5' end (blue) threaded through the center of a 3-helix junction (3' labeled red). The pseudoknot forms a mechanical barrier which prevents progression of the 5'→3' exonuclease XRN1 (PDB 5TPY, adapted from Akiyama et al., 2016).

1.3.1   S. *cerevisiae* Genomics

The S. *cerevisiae* genome is 12,068 kilobases long and encoded 5885 proteins, 140 ribosomal RNAs, 40 small nuclear RNAs, and 275 transfer RNAs, all found within the yeast's 16 chromosomes (Goffeau et al., 1996). The reference genome is S288C, which is stored in the *Saccharomyces* Genome Database (https://www.yeastgenome.org) and has a genotype of *MATα SUC2 gal2 mal2 mel flo1 flo8-1 hap1 ho bio1 bio6* (See below) (Mortimer and Johnston, 1986).

Cells can be either haploid or diploid, and both types of cells can reproduce asexually by mitosis through budding, a process through which a daughter cell buds off a mother cell. Haploid cells can also reproduce sexually by mating with cells of the opposite mating type. The two different type of cells, **a** and **α**, produce mating pheromones called **a**-factor and **α**-factor, respectively. Each mating type can only respond to the opposite mating pheromone, and the **a-**type cells respond to the presence of the **a**-factor by growing a projection called a shmoo toward the source of the mating factor. In contrast, diploid cells can undergo meiosis and sporulation under conditions of stress, producing four haploid spores, two of each mating type, which can subsequently reproduce sexually (For review, see Duina et al., 2014; Billard et al., 2012).

By convention, yeast gene symbols contain three italic lowercase letters followed by an Arabic number of the identifying mutation, and uppercase identifies a dominant gene while a lowercase identifies a recessive gene. Alleles are listed as the gene symbol, followed by a hyphen and an italic Arabic number. Alleles that have been altered recombinantly are listed by the gene symbol followed by a specification on the type of

20

alteration performed: (::) for a disruption, (-Δ) for a deletion, and (Δ::) for a replacement. Proteins are written as the gene symbol, non-italicized, with the first letter uppercased, and followed by the suffix "p". Phenotypes are listed as the non-italic three letters of the gene symbol (first letter uppercase), followed by a superscript "+" sign for wild-type and "-" sign for mutant. When listing the genotype, the mating type loci are normally listed first, followed by the gene symbols of the mutated and recombinant genes (Cherry, 1998).

1.3.2   Auxotrophy as a Selective Marker

Auxotrophy refers to the inability of a particular organism to synthesize a metabolite needed for its growth and reproduction. By definition, the wild-type (WT) strain is a prototroph, indicating that it can synthesize all the nutrients required for its survival. Through a mutation in a key gene, a new mutant strain can be created that enables for auxotrophic selection. For example, the *ura3-52* mutation, caused by an insertion of the transposable element Ty into the coding region of the *URA3* gene encoding for Orotidine 5'-phosphate decarboxylase (ODCase), transforms the mutant cells into uracil auxotrophs (Rose and Winston, 1984; Flynn and Reece, 1999). If a plasmid containing the *URA3* ORF is used to transform these auxotrophs, only the cells that were successfully transformed with the plasmid will be able to grow in minimal media lacking the amino acid uracil, thus enabling selection of the desired cells.

1.3.3   IRES in Yeast

Although many functioning eukaryotic IRES elements had been found, successful

internal ribosomal entry had not been reported in yeast until Thompson *et al*. (2001)

reported efficient translation of the second gene in a bicistronic reporter in S. *cerevisiae*,

through the use of the CrPV IRES. Although the authors reported poor translation

efficiency in WT cells, they found that cap-independent translation was markedly

increased in the H2545 strain (Dever et al., 1995), which contains disrupted *imt3* and

imt4 genes, encoding for two initiator tRNAs. Disrupting expression of these two

tRNA^{met} genes decreases the intracellular concentration of the eIF2•GTP•Met–tRNA$_i^{Met}$

ternary complex, enhancing the rate of cap-independent translation.

1.4   THESIS OBJECTIVE

This work focuses on the investigation of the effect of artificially-installed

xrRNAs into previously-characterized splicing reporters (Mayas et al., 2010), through

transformation of S. *cerevisiae* cells with reporters with and without functioning xrRNAs

and IRES elements. *In vivo* assays examine enzymatic activity in the cells, as well as

quantify relative protein and RNA transcript content upon transformation with the

different reporters. Through these experiments designed to prove the behavior of the

reporters, this work aims to answer the fundamental research question of whether

mRNAs containing artificially-installed xrRNAs can be translated into protein, and

whether they lead to accumulation of decay-resistant transcript and increased levels of

protein expression. The reporter of choice is a bicistronic plasmid containing the *ACT1*

22

gene (and its intron), followed by the *LACZ* gene. The reporter also contains the *URA3*

gene as a marker. The xrRNAs have been inserted into the intergenic region, followed by

the CrPV IRES. The two viral elements are hypothesized to be able to work in tandem, to

allow cap-independent translation of the decay-resistant mRNA fragments (FIGURE 6).
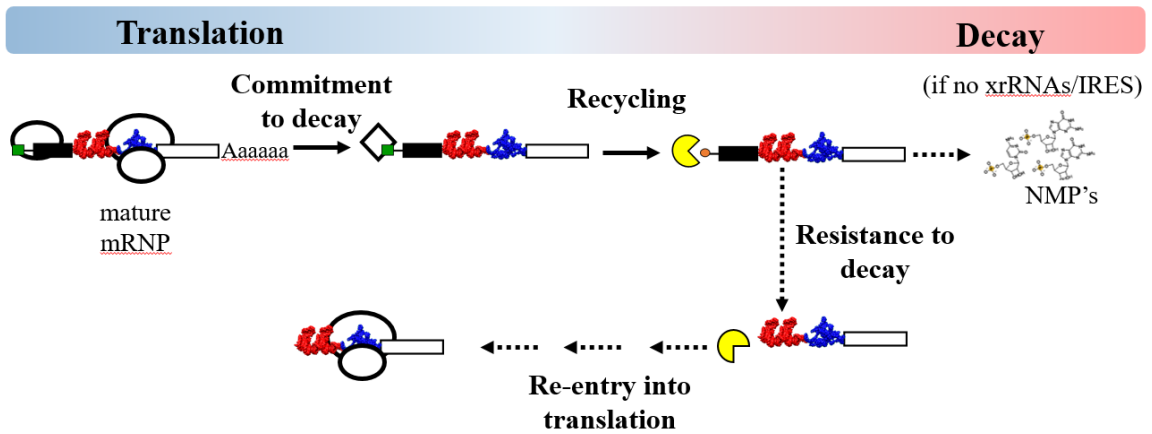
FIGURE 6. Translation of partially-decayed messenger RNAs. Addition of the decay-resistant structures (xrRNAs) to the reporters should result in accumulation of partially-decayed transcripts. Since these transcripts contain the CrPV IRES structure to allow for cap-independent translation, translation of partially-decayed mRNAs should result in increased protein synthesis.

1.4.1   Research Aim 1. Detection of Decay-Resistant Transcripts

RNA transcripts can be quantified directly through primer extension followed by

fragment analysis through capillary electrophoresis. Reverse transcription is initiated by

landing a complementary fluorescently-labeled DNA primer onto the RNA transcripts.

After extension by an RNA-dependent-DNA-polymerase and subsequent degradation of

remaining RNA, complementary DNA (cDNA) is obtained. The cDNA can be analyzed

through capillary electrophoresis. After applying an electric field to the capillary, cDNA

will travel to the positive electrode with a speed reversely proportional to its length. Detection of the fluorescently labeled cDNA and integration below the curve of the corresponding peaks allows for quantification of the nucleic acid at each detected length.

1.4.2   Research Aim 2. Quantification of Enhancement in Protein Expression

Since the LACZ gene is located downstream from the xrRNAs, the protective effect of these structures from the decay machinery can be examined by comparing the transcription of the gene in cells expressing reporters with and without the xrRNAs. Furthermore, since the IRES element should allow for cap-independent translation of the β-galactosidase enzyme encoded by *LACZ*, protein expression of β-galactosidase can be quantified and compared. The activity of β-Galactosidase is commonly quantified through the β-Galactosidase assay. *In vivo*, β-Galactosidase is responsible for cleaving lactose into glucose and galactose. The compound o-nitrophenyl-β-D-galactoside (ONPG) is also recognized as a substrate and is cleaved into galactose and o-nitrophenol, which has an observable yellow color and absorbs light at 420 nm. This allows for both qualitative and quantitative examination of β-Galactosidase activity in vitro. When cell lysates are incubated with excess ONPG, the production of o-nitrophenol over time is proportional to the concentration of β-Galactosidase. This is quantifiable through the absorbance at 420 nm and normalized by time and initial cell concentration.

While the β-Galactosidase assay can be used to quantify enzymatic activity, which should be proportional to protein concentration, protein content can be directly measured through western blotting. Analysis of whole protein cell content can be

performed by lysing the cells in order to solubilize cellular proteins in a lysis buffer, which can subsequently be ran through a gel in order to separate all the proteins by size using gel electrophoresis. After transfer of the proteins from the gel to a nitrocellulose membrane, the whole cell protein lysate can be examined for the content of a specific protein using target-specific antibodies. Through the use of a primary antibody specific to β-galactosidase, followed by a fluorescently-labeled secondary antibody specific to that primary antibody, the presence of β-galactosidase can be detected. This allows for the semi-quantitative analysis of relative protein content with the reporters with and without the decay-resistant structures.

CHAPTER 2: MATERIALS AND METHODS

2.1   <u>Strains and Plasmids.</u>

Strain	Relevant Genotype	Parental Strain	Reference or source
S288C	*MATα SUC2 gal2 mal2 mel flo1 flo8-1 hap1 ho bio1 bio6*		Mortimer and Johnston, 1986
H2545	*MATa trp1-D1 ura3-52 IMT1 IMT2 imt3::TRP1 imt4::TRP1 leu2::hisG GAL1*		Thomspon et al., 2001; Dever et al., 1995
CRY1	*MATa ade2-1 can1-100 his3-11,15 leu2-3,-112 trp1-1 ura3-1*	W303-1A	Cherry et al., 2019; Brickner & Fuller, 1997
YJH632	*MATa ade2-1 can1-100 his3-11,15 leu2-3,-112 trp1-1 ura3-2, xrn1Δ::HygMX*	CRY1	Cherry et al., 2019
YJH898	*MATa ade2-1 can1-100 his3-11,15 leu2-3,-112 trp1-1 ura3-3, dxo1Δ::KanMX*	CRY1	Cherry et al., 2019
YJH867	*MATa ade2-1 can1-100 his3-11,15 leu2-3,-112 trp1-1 ura3-4, xrn1Δ::HygMX, dxo1Δ::KanMX*	CRY1	Cherry et al., 2019

TABLE 1. Strains used.

Yeast parental strain S288C was purchased from Fisher Scientific and

manufactured by GE Dharmacon™ (Dharmacon catalog # YSC1060) and was used as a

reference strain for all knockout-confirmation colony PCR experiments. Strain H2545

was used for all protein expression experiments utilizing the JPS 1480 series reporters, as

well as fragment analysis. β-Galactosidase assay was also performed on CRY1 strains

(Obtained from Patrick D. Cherry) and its derived mutants expressing the JPS 1480 series

reporters (TABLE 1).

Plasmid	Element		
	xrRNAs	CrPV IRES	*LacZ*
JPS 1481	No	Yes	Yes
JPS 1481X	Yes	Yes	Yes
JPS 1481M	Inactive	Yes	Yes
JPS 1482	No	Inactive	Yes
JPS 1482X	Yes	Inactive	Yes
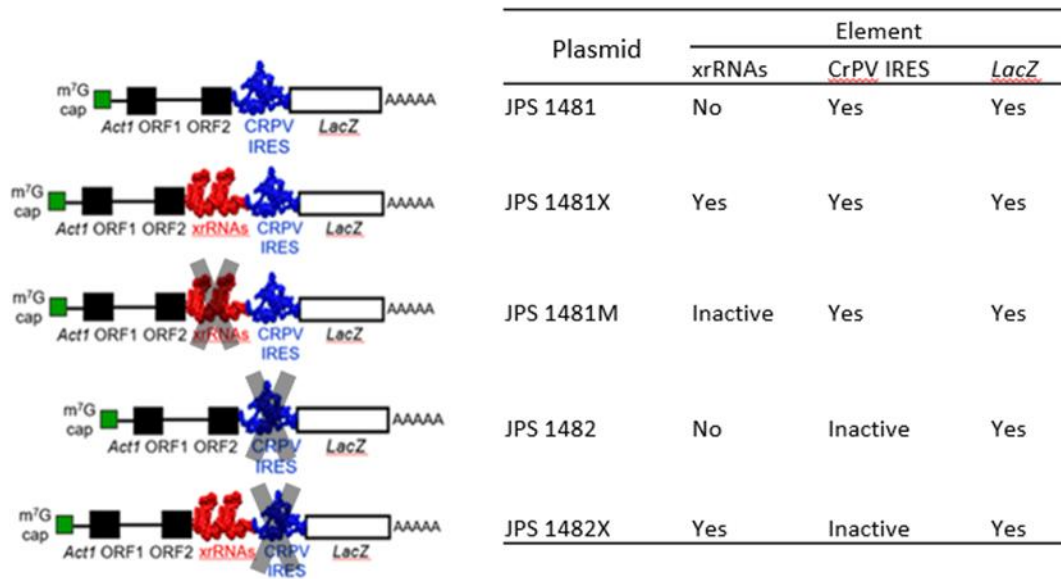
FIGURE 7. JPS 1480 series reporters. All plasmids were kindly provided by the
Jonathan P. Staley lab.

JPS 1480 series reporters (FIGURE 7) were obtained from Jonathan P. Staley's

lab (Mayas et al., 2010). All reporters are bicistronic and include a 5' m7G cap, the *Act1*

gene, and the CrPV IRES followed by the *LacZ* gene and a poly(A) tail (JPS 1481). In

addition, the JPS 1481X reporter contains the xrRNAs immediately preceding the CrPV

IRES. The JPS 1481M reporter contains the sequence for the xrRNAs but with a 3-

nucleotide mutation along each of the two copies of the pseudo-knots (FIGURE 9) which

27

prevent the proper folding of the structures. The JPS 1482 and 1482X reporters contain a 2-nucleotide mutation along the IRES, which render the IRES inactive (FIGURE 2, 9).

2.2   Yeast Husbandry.

All cells were incubated at 30 °C. Liquid cultures were incubated for the specified amount of time, and all cultures on the surface of plates containing solid media, unless specified, were grown for 2-3 days. Strain H2545 was grown in complex Yeast Peptone Dextrose media (YPD), containing 1 g/L bacto yeast extract, 2 g/L peptone, 2 g/L d-glucose (dextrose), and 2 g/L agar (for plates only). Solutions were sterilized by autoclaving. Strains S288C and CRY1 were grown in complex YPD plus Adenine media (YPAD, which has the same composition of YPD plus 0.004% adenine sulfate (supplementation with adenine inhibits reversion of *ade1* and *ade2* mutations present in CRY1 cells, which cause red coloration on the yeast colonies. Dorfman, 1969). CRY1 knockout strains were grown YPD media supplemented with either 200 µg/mL Hygromycin B for *XRN1* knockouts, or 300 µg/mL G18 for *DXO1* knockouts (or both for ∆*XRN1*/∆*DXO1*).

Uracil auxotrophic strains expressing the JPS 1480 series reporters were grown in Synthetic Defined media containing 2% d-glucose and lacking uracil (SD/-ura). Composition of SD/-ura is 5 g/L ammonium sulfate, 1.7 g/L yeast nitrogen base without amino acids, 2 g/L drop out synthetic mix (-his, -leu, -trp, -ura) without yeast nitrogen base (US Biological cat. #D9540), 40 mg/L tryptophan, 160 mg/L leucine, 20 mg/L histidine, and 2 g/L agar for plates. Solutions without amino acids or sugar were

28

autoclaved, and supplemented with sterile-filtered stock solutions (4 mg/ml tryptophan solution, 8 mg/ml leucine solution, 4 mg/ml histidine, 20% (w/v) glucose). Note that if uracil is added to SD media, it is to a concentration of 20 mg/L.

2.3   Transformation of Yeast Cells

Starter cultures were inoculated with the empty or WT cells and incubated overnight at 30 °C in 5 mL of the appropriate media (either YPD or YPAD). The overnight culture was used to seed a new 50 mL culture, which was grown to mid-log phase. The cells were pelleted at 3068 rcf for 10 minutes and supernatant was discarded. Cells were resuspended in 50 mL Molecular Biology Grade water (MBG H_2O) and pelleted at 3068 rcf for 10 minutes. After discarding supernatant, cells were resuspended in 500 µL 100 mM lithium acetate. Suspension was spun down and supernatant was discarded. Cells were resuspended in 50 µL MBG H_2O and 10 µL salmon sperm DNA were added to spurn recombination. Approximately 1 µg of plasmid DNA was added, followed by 500 µL PLATE (40% PEG 3350, 100 mM LiOAc, 10 mM TRIS7.5, 0.4 mM EDTA). The tubes were vortexed to homogenize and heated to 42 °C for 35-40 minutes. The resulting mixture was used to streak plates containing the selection media, SD/-ura.

2.4   Sequencing

Plasmids were isolated from DH5α E. coli. competent cells previously transformed with each of the reporters. 5 mL bacterial cultures of LB media (10 g/L tryptone, 5 g/L yeast extract, and 5 g/L NaCl) supplemented with either 200 µg/mL

29

Primer Name	Description	Sequence (5'-3')
New LacZ PE	*LacZ*, front end, reverse	CCAGGGTTTTCCCAGTCAC
EC JPS series 1480 primer 3	CrPV IRES, forward	GCTATTTAGCTTTACGTTCCAGG
Ana001	*ACT1* intron, front end, reverse	CTCTCGAGCAATTGGGACCG
Ana002	*LacZ*, Back end, forward	CGGATTGATGGTAGTGGTCAAATGG
Ana003	Cup1, Back end, forward	CGACGATTCTACTCAGTTTTGAGTACAC
Xrn1(YGL173C)B	*XRN1*, front end (base 122), reverse	TGTAAAATCGAATTCATATCCAGGT
D208R3	*XRN1*, front end (base 610), reverse	CGTAAATACAATGTCTCGTATTCTGG
XRN1 base 1190	*XRN1*, front end (base 1190), forward	GGTTGATGGAGCAATTAC
W543-R-AJ	*XRN1*, front end (base 1616), reverse	TCAACGTAGTCTTTAGCAAG
Xrn1-Base3034-AF	*XRN1*, back end (base3034), forward	GGGAAGCATATCAATGTTGGTATCCC
Xrn1-Base3924-AF	*XRN1*, back end (base3924), forward	GGGATCGCAAAAAGATTCCAAACCC
Xrn1(YGL173C)C	*XRN1*, back end (base 4362), forward	AGATCAAGGAAGTCGTATTGTTGTC

TABLE 2. Primers used for sequencing of JPS 1480 series reporters and pXRN1 (BJH 872).

ampicillin (for all JPS 1480 reporters) or 100 µg/mL kanamycin (for BJH 872) for selection, were incubated overnight at 37 °C. Plasmid DNA was isolated using the ZR Plasmid Miniprep-Classic Kit obtained from Genesee Scientific (Catalog # 11-308A) and following the protocol specified in the kit. The resulting plasmid was diluted to a concentration of approximately 80 ng/ µL and mixed with 5 µL of primer at a concentration of 5 µM (TABLE 2). The samples were submitted for sequencing to Quintara Biosciences. Data obtained was analyzed using SnapGene®.

2.5   Colony PCR

Cells were grown in the appropriate solid media and incubated at 30 °C for 3 days, until large colonies formed. One large colony (≈1-2 mm in diameter) was suspended in 50 µL lysis buffer (1% Triton-X 100 (v/v), 20 mM Tris-HCl pH8.5, and 2 mM EDTA in MBG H$_2$O) and heated at 95 °C for 10 minutes. Samples were centrifuged at 18,407 rcf for 10 minutes to remove cellular debris, and supernatant was transferred to a new tube. The resulting lysate was used as a template for each PCR reaction.

Target	Direction	Sequence (5'-3')
imt3	Forward	GGATTTCATTCTAACACAGCTCAGTGTGC
imt3	Reverse	CCATTAATGAAGTGTTCTATATTGAGGC
imt4	Forward	GCGACATGGAGAGATAGAGATAGAAGAATTTG
imt4	Reverse	CAATTATTAATAATAACGCAGAAGTTAAAGC
XRN1	A-Forward	CCTCCTTTGCTCGTCTTTTCGCCACCACC
XRN1	C-Forward	TTCCAATCATAGGAGAAAACTTCTG
XRN1	D-Reverse	GCGGAAAGCTTTGTGTAAAAAATACCC
DXO1	A-Forward	GGCATTGTTGCATTACAGCGCCAG
DXO1	D-Reverse	GCCATCTTCCAATGTATTCTGGTATCG

TABLE 3. Primers used for colony PCR knockout-confirmation experiments.

PCR reactions were setup containing: 4 µL of lysate, 2.5 µL 10 mM forward primer, 2.5 µL 10 mM reverse primer, 20 µL 1.25 mM dNTP mix, 10 µL 5X HF buffer (ThermoFisher Scientific catalog #F520L), 50 mM $MgCl_2$ (ThermoFisher Scientific catalog #F518L, to a final concentration of 4 mM), 2.5 µL 0.5 µL 10% Phusion High-Fidelity DNA Polymerase (v/v) (ThermoFisher Scientific catalog #F530L), and MBG H_2O to a final volume of 50 µL. Primers used for each template are listed on TABLE 3. PCR amplification was performed in a thermal cycler programmed at 98 °C for 3 minutes for initial denaturation; followed by 35 cycles of denaturation at 98 °C for 30 seconds, annealing for 30 seconds at a temperature gradient of 55-70 °C, and extension at 72 °C for varying lengths of time for each template; and finalized by extension at 72 °C for 7 minutes. Extension time was 30 seconds for *imt3* and *imt4*, 3 minutes 30 seconds for XRN1, and 1 minute 30 seconds for DXO1. PCR products were mixed with 10 µL of 6X loading dye, and separated by electrophoresis at 100V for 1 hour in a 1% (w/v) agarose gel in Tris-Acetate-EDTA (TAE) buffer containing 0.5 µg/mL ethidium bromide. Gels were visualized using the Bio-Rad ChemiDoc™ MP Imaging System. Image was analyzed using Bio-Rad Image Lab™ 6.0 Software and labeled using Microsoft® PowerPoint®.

2.6   Quantification of Enhancement in Protein Expression

2.6.1 β-Galactosidase Assay

Cells were grown to OD600≈0.5 in the appropriate media. 1.5 ml aliquots were pelleted and washed with Z-buffer (60 mM Na_2HPO_4, 40 mM NaH_2PO_4, 10 mM KCl, 1

mM MgSO$_4$; pH 7.0). Pellet was resuspended in 100 µL of Z-buffer and subjected to

lysis through 6 cycles of freeze-thawing (freezing on liquid N$_2$ followed by thawing in

42°C water bath). Reaction was started through the addition of 700 µL of Z-buffer

containing 1 mg⁄mL ortho-nitrophenyl-β−galactopyranoside and 50 mM β-

mercaptoethanol. After incubation at 30 °C for 3 hours, reaction was quenched by adding

of 500 µL 1M Na$_2$CO$_3$. Cell debris was pelleted and absorbance of the supernatant was

measured at 420 nm using the Tecan Infinite® M1000 plate reader (also used to measure

the initial OD600). Measurements were corrected for activity in wild-type cells and

Miller units were calculated using EQUATION 1 (Miller, 1972).

$$(\text{EQUATION 1}) \qquad Miller\ Units = \frac{OD420\ x\ 1000}{OD600\ x\ Time\ (min)x\ Vol\ (mL)}$$

2.6.2   Western Blots

Extraction of total yeast cellular protein content was performed as previously

described (Kushnirov, 2000). Specifically, cell cultures were grown to OD600≈0.5, from

which 4-6 mL aliquots were harvested and pelleted by centrifugation. Pellets were

washed with 500 µL of ice-cold water, pelleted and resuspended in 100 µL of water.

Cells were lysed by addition of 100 µL of 0.2 M NaOH and incubation at room

temperature for 10 minutes. Cells were centrifuged at 15,871 rcf for 30 seconds and

supernatant was discarded. Pellet was resuspended in 50 µL of 2x Laemmli Sample

Buffer obtained from Bio-Rad, and 30 µL aliquots were loaded for separation by SDS-

page. After electrophoresis, proteins were transferred to a nitrocellulose membrane and

immunoblotted with a rabbit β-galactosidase specific antibody (Novus Biologicals

catalog number NB300-327) and a rabbit GAPDH specific antibody as a loading control (Novus Biologicals catalog number NB300-327). Blots were then incubated with a goat anti-rabbit IgG antibody labeled with StarBright™ Blue 700 dye (Bio-Rad catalog number 12004162). Detection was performed using the Bio-Rad ChemiDoc™ MP Imaging System. Image was analyzed using Bio-Rad Image Lab™ 6.0 Software and labeled using Microsoft® PowerPoint®.

2.7 Detection of Decay-Resistant Transcripts

2.7.1 Fragment Analysis of Primer Extension Products

RNA isolation was performed from cells grown to OD600 between 0.5 and 0.7 and pelleted by centrifugation at 3068 rcf at 4°C. Cells were resuspended in 1000 µL of cold DNase/RNase-free H_2O. Cells were centrifuged for 1 min at 6010 rcf, supernatant was removed and pellet was frozen on liquid N_2. Pellet was thawed on ice and resuspended in 400 µL cold TES. 400 µL warm acid phenol was added, after which samples were vortexed for 15 seconds and incubated at 65°C for 30 minutes while vortexing for 15 seconds every 5 minutes. Samples were transferred to ice and incubated for 5 minutes, then centrifuged at 1503 rcf at 4°C for 10 minutes. Aqueous (top) layer was transferred to a new tube and 400 µL chloroform was added. After vortexing for 15 seconds, samples were centrifuged at 18,407 rcf at 4°C for 10 minutes. Aqueous layer was transferred to a new tube and 40 µL 3M sodium acetate and 1000 µL 100% ethanol were added. Tubes were inverted to mix and incubated at -80°C for at least 20 minutes. After incubation, samples were centrifuged at 15,871 rcf at 4°C for 8 minutes.

Supernatant was carefully removed by micropipette and pellet was washed by adding cold 70% ethanol and inverting to mix. Samples were again centrifuged at 15,871 rcf at 4°C for 8 minutes and supernatant removed by micropipette. Tubes were inverted and allowed to fully dry for around 30-60 minutes. The pellet (containing isolated RNA) was resuspended in 50 µL of DNase/RNase-free molecular-grade H_2O, heating to 65°C for 5 minutes if needed. The RNA was stored at -80°C.

The yeast total RNA was diluted to a concentration of 400 ng/µL and reverse-transcribed. 12.5 µL of the yeast RNA was mixed with 2.5 µL hybridization mix (3.75 µM reverse-transcription primer labeled with 6-FAM dye in 200 mM Tris pH 8, 200 mM NaCl, 40 mM DTT, can add 1.25 µM of a secondary primer as a loading control). Reverse transcription primer used was New LacZ PE (FIGURE S1, TABLE 2). Mixture was folded in the themocycler: 90°C for 3 minutes, 55°C for 3 minutes, 4°C hold. Samples were removed and frozen on liquid N_2. 1 µL GoScript™ Reverse Transcriptase (Promega, catalog number A5003) and 14 µL RT mix (1.6 mM each dNTP, 10 mM $MgCl_2$, 167 mM Tris pH 8.3, 17mM DTT, 250 mM KCl) were added. Reverse transcription was performed in the thermocycler: 42°C for 45 minutes, 55°C for 15 minutes, 65°C for 15 minutes, 20°C hold. After reverse-transcription, remaining RNA was degraded by the addition of 3 µL 100 mM NaOH and incubation at 90°C for 3 minutes. Samples were spun down and purified on a G-25 sephedex column (10%w/v beads in H_2O). 25 µL formamide was added and samples were sent for fragment analysis to GeneWiz (Applied Biosystems™ GeneScan™ 600 LIZ™ dye Size Standard added by GeneWiz), or Quintara Biosciences. Capillary

electrophoresis analysis performed by Quintara Biosciences were performed with either

pre-added ROX 1000 ™, or 600 LIZ™ dye size standard added by Quintara Biosciences

(Both size standards by Applied Biosystems™ GeneScan™). Fragment analysis data was

analyzed using Applied Biosystems™ Peak Scanner™.

CHAPTER THREE: RESULTS

3.1   <u>Vector Composition</u>

The sequencing results confirmed the presence of all the key elements in the

reporter vectors, shown in FIGURE 8 and FIGURE S1. All vectors feature the

constitutively active, 643-bp-long GAP promoter, followed by the *ACT1* gene totaling

394 base pairs, made up of a 5' UTR, and ORFs A and B separated by an intron. The

ACT1 ORF B is followed by a very short non-coding region (11 bp), which is where the

xrRNAs were inserted into 1481X, 1481M, 1482X and 1482M vectors. The xrRNA

element is composed of two adjacent pseudoknot structures totaling 173 bp in length.

This region is followed by the CrPV IRES element in all the reporter vectors, which is

192 base pairs long and is immediately followed by the *Lac*Z gene. The *Lac*Z ORF is

3,066 bp long and was not fully sequenced. The 5' and 3' ends of the ORF were

confirmed by sequencing, but approximately 2,400 bp were left unsequenced. The

remaining sequence (FIGURE 8) was approximated based on homology and assumed to

be present due to the confirmed enzymatic activity in the cells expressing the reporters

(FIGURE 13) and detection of β-galactosidase with protein-specific antibodies (FIGURE

12), confirming the presence of the fully-functioning protein. The *CUP1-1* ORF (182 bp) that follows is in frame with *LacZ* and is in turn followed by a non-coding region and the *PGK1* terminator, encoding redundant polyadenylation signals.
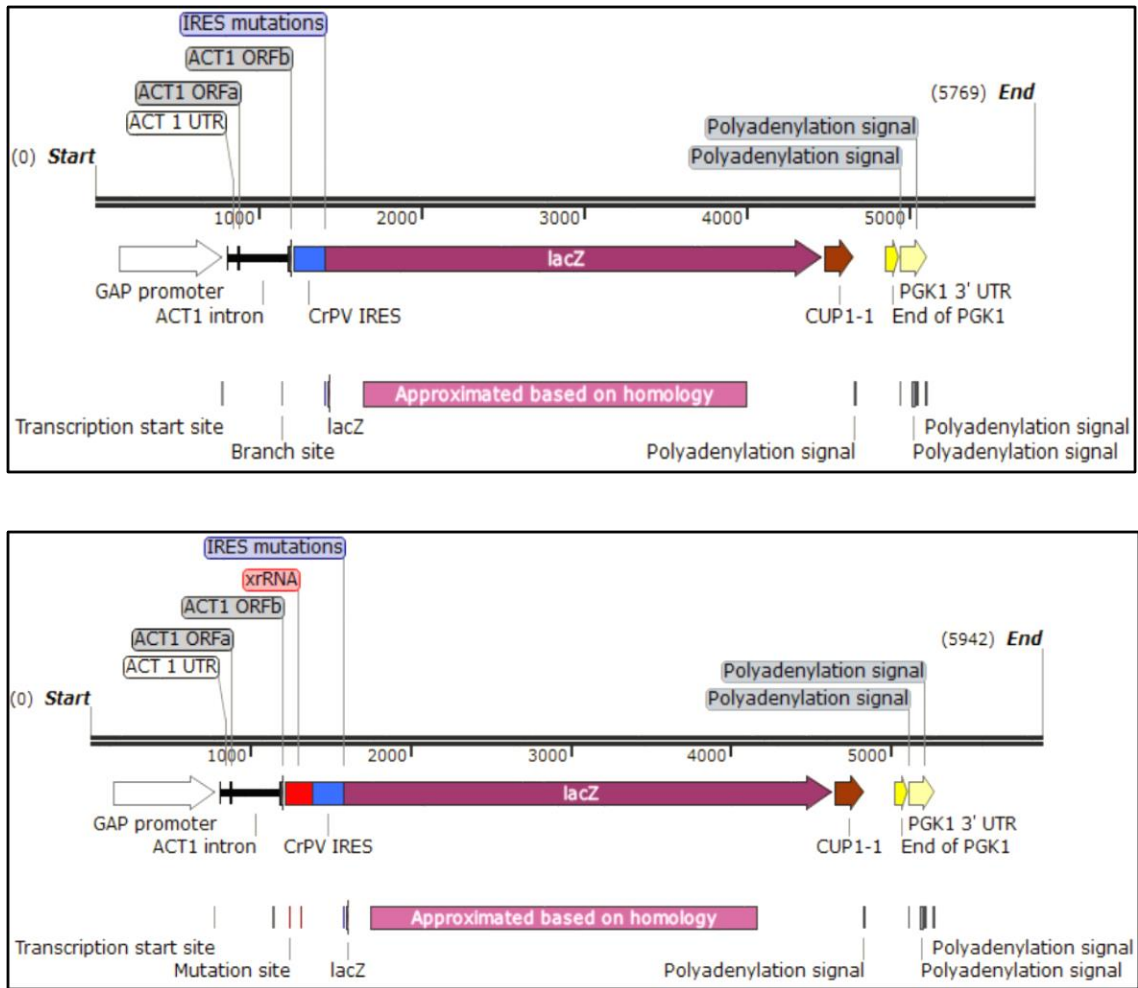
FIGURE 8. Map of reporter vectors JPS 1481 (top) and 1481X (bottom), containing all key features. All reporters contain the following elements, listed in the 5'→3' direction: the GAP promoter (white arrow), *ACT1* (black), CrPV IRES (blue), *LacZ* (magenta), *CUP1-1* (brown), and the *PGK1* terminator (yellow). In addition, all reporters designated as "X" or "M" contain the xrRNAs (red), located between *ACT1* and the CrPV IRES.

The point mutations corresponding to each mutant structure were also confirmed by sequencing (FIGURE 8, 9). Each of the two copies of the pseudoknot structure in the xrRNAs contains a triplet in which each base was mutated to its corresponding canonical Watson-Crick complementary base (AGT→TCA), generating the mutant structure encoded in JPS 1481M. Similarly, the IRES-dead mutants (1482 and 1482X) contain a CC→GG mutation toward the end of the structure, which was confirmed by sequencing.

xrRNAs	1481X (1-35)	AGGCAAAACTAACATGAAACAAGGCTAAA**AGT**CAG
	1481M (1-35)	AGGCAAAACTAACATGAAACAAGGCTAAA**TCA**CAG
	1481X (87-121)	CAAGGACGTTAAAAGA**AGT**CAGGCCATCACAAATG
	1481M (87-121)	CAAGGACGTTAAAAGA**TCA**CAGGCCATCACAAATG
IRES	1481 (158-192)	AGATTAGGTAGTCGAAAAACCTAAGAAATTTA**CC**T
	1482 (158-192)	AGATTAGGTAGTCGAAAAACCTAAGAAATTTA**GG**T

FIGURE 9. Sequence alignments of the different JPS 1480 series reporters confirming the presence of point mutations in the mutant structures. The mutant xrRNAs contain AGT→TCA mutations in bases 30-32 and 103-105 (shown in red, 1481M), and the mutant CrPV IRES contains a CC→GG mutation in bases 190-191 (shown in blue, 1482 and 1482X).

3.2   Methionine Initiator tRNA Genes are Knocked-Out in H2545 Strain

The H2545 laboratory yeast strain was chosen for the investigation of the JPS 1480 series reporters because it had been previously reported to allow for successful cap-independent translation (Thompson et al., 2001). The H2545 strain was constructed from an ascospore cross between two strains, each containing a mutation that inactivated one of the four *IMT* (methionine initiator tRNA) genes encoded in the WT strain S288C (Byström and Fink, 1989; Dever et al., 1995). The resulting H2545 strain thus contains

two knocked-out *IMT* genes, *imt3* and *imt4*. Deletion of these two genes limits the

availability of the eIF2•GTP•Met–tRNA$_i^{Met}$ ternary complex in the cell, therefore

reducing the rate of cap-dependent translation and allowing the CrPV IRES to effectively

compete for the translation machinery (Thompson et al., 2001).
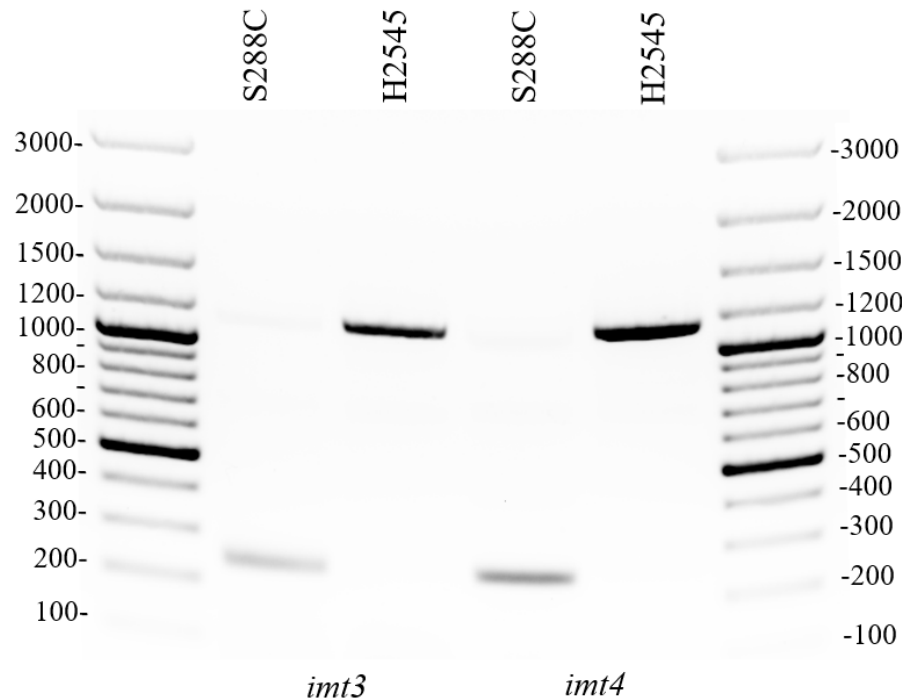
FIGURE 10. Colony PCR results confirming that *imt3* and *imt4* genes are knocked-out in H2545 yeast, priming that strain for successful cap-independent translation of the bicistronic reporter. Large individual colonies of S288C and H2545 were resuspended in lysis buffer and lysed by heating to 95 °C. Lysates were used as templates for PCR amplification using *imt3*- and *imt4*-specific primers and subjected to equal reaction conditions. PCR products were analyzed through gel electrophoresis and examined for presence of bands at different lengths between the two strains.

In order to experimentally verify that the two initiator methionine genes (*imt3* and

imt4) are knocked-out in the H2545 strain, cells were subjected to colony PCR analysis

and compared to the reference strain S288C. The genomic DNA of the H2545 and S288C

40

strains was isolated and analyzed via PCR using target-specific primers designed to amplify the full *imt3* and *imt4* ORFs. In the WT reference sequence (S288C), PCR amplification with the designed primers leads to products that are 241 and 247 base pairs long for *imt3* for *imt4* respectively. Each *imt* ORF IS 72 BP long and contains a *Bss*HII site at position 21, which was digested and used to create the mutants. The restriction site was filled in with deoxynucleotides, then blunt-end ligated to phosphorylated *Xho*I linkers. Similarly, the full *TRP1* gene (675 bp long) was obtained by digestion of the *Eco*RI-*Bss*HII fragment (890 bp long), which was also filled with deoxynucleotides and blunt-end ligated to phosphorylated *Xho*I linkers. The two fragments were digested at the *Xho*I site and linked together, resulting in disruption of each *imt* ORF with the *TRP1* gene (Byström and Fink, 1989). This leads to mutant cells with inactive *imt3* and *imt4* genes, but a fully-functioning copy of the *TRP1* gene. PCR amplification of the knockout mutants should result in products with an increased fragment length using the *imt3-* and *imt4*-specific primers, at 1133 bp and 1139 respectively. The colony PCR experiments results confirm that both methionine initiator tRNA genes are knocked out in the H2545 strain (FIGURE 10).

3.3   Expression of Reporters Containing xrRNAs Yields Decay-Resistant Transcripts

          In order to determine if the addition of xrRNAs to the reporters resulted in the accumulation of decay-resistant fragments, RNA was isolated from whole cell lysates and subjected to reverse transcription and subsequent fragment analysis by capillary

electrophoresis. Fragment analysis of cell cultures with the different JPS 1480 series

reporters showed the presence of decay-resistant transcripts containing one and two
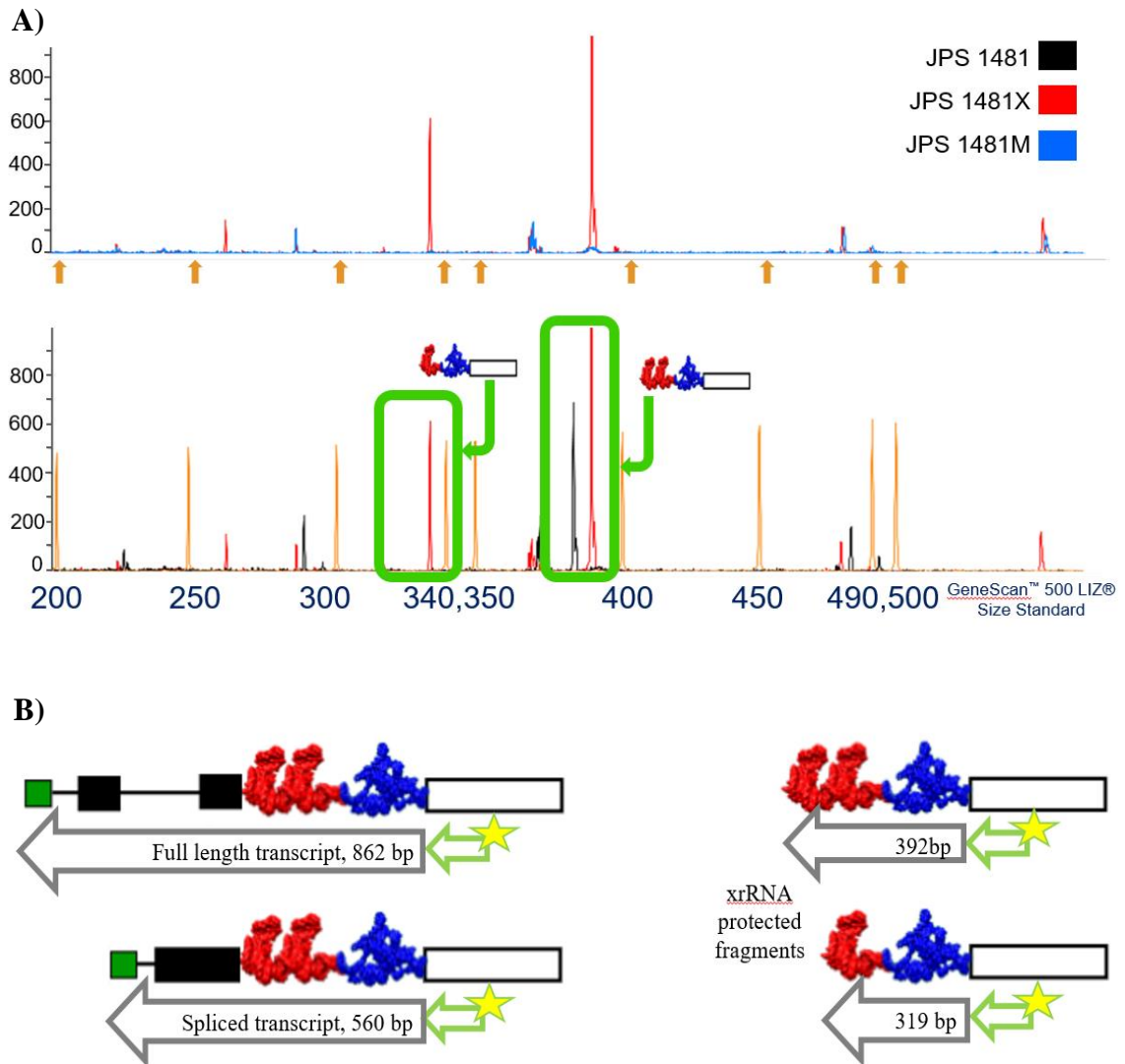
FIGURE 11. **A)** Fragment analysis data showing the presence of transcripts protected from degradation by one and two copies of the xrRNAs (shown by green box). MW size standard shown as orange peaks, and corresponding lengths (bp) of the standard peaks are indicated by black arrows **B)** Expected fragment length of transcripts containing the xrRNAs. Total yeast RNA content was isolated and reverse-transcribed using a fluorescently-labeled primer. The resulting fluorescently-labeled cDNA fragments were analyzed by capillary electrophoresis. The green arrow illustrates the approximate binding site of the primer. Results confirm the accumulation of xrRNA-protected fragments.

copies of the Xrn1-resistant structures, at around 319 and 392 bp respectively, in cells

expressing the JPS 1481X reporter (FIGURE 11). The decay-resistant transcripts were

detected only in the cells expressing the reporter containing the fully-functioning xrRNAs

(red), and not in the mutant (blue), or in the reporter lacking the structure altogether

(black). These xrRNAs, indicated by the green boxes, appear to accumulate in the cells,

as evidenced by the height of the xrRNA protected fragments relative to the height of all

the other peaks of the same color.
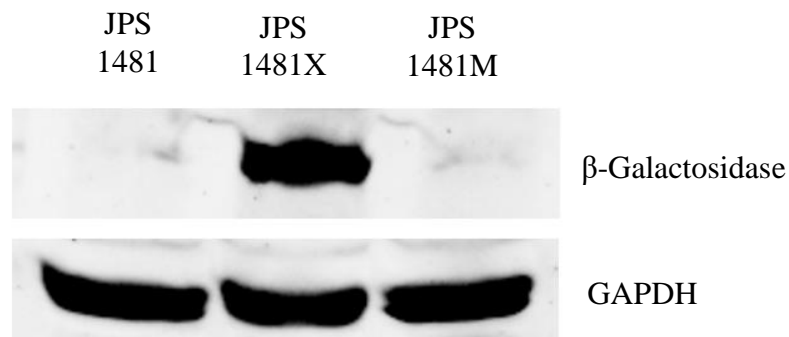
FIGURE 12. Western Blot of H2545 cells expressing three different reporters
from the JPS 1480 series. Whole cell protein extracts were incubated with either anti-β-
Galactosidase or anti-GAPDH primary antibodies. A prominent band corresponding to
the molecular weight of β-Galactosidase was observed in the cells expressing the
reporter containing the fully-functioning xrRNAs (1481X), but no significant bands
were observed if the reporter was lacking the xrRNAs (1481) or contained the mutant
copy (1481M). This confirms that addition of the xrRNAs leads to increased protein
expression of the target protein.

	JPS 1481	JPS 1481 X	JPS 1481 M	JPS 1482	JPS 1482 X
xrRNAs		+	-		+
IRES	+	+	+	-	-
LacZ	+	+	+	+	+
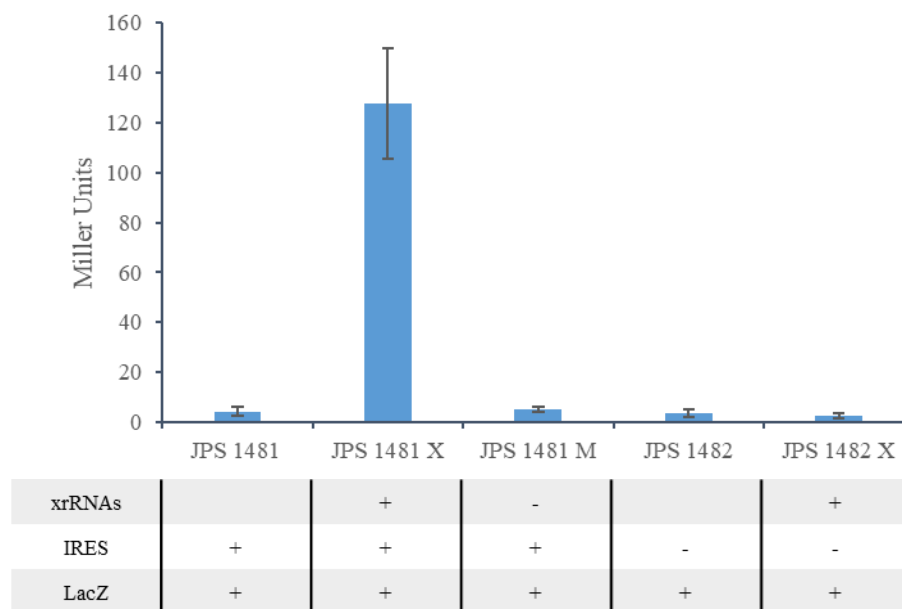
FIGURE 13. Enzymatic activity of β-galactosidase in cell cultures expressing different reporters from the JPS 1480 series. Total yeast protein lysates were incubated with ONPG for 3 hours. Enzymatic activity was quantified as absorbance at 420 nm and normalized for reaction time and initial cell concentration, measured as absorbance at 600 nm. The reporters include either the active form of each element (+), the mutant or inactive form (-), or are missing the element listed (left blank). Increased enzymatic activity is only observed upon transformation with reporters with fully-functioning copies of both xrRNAs and IRES.

3.4   Partially-Decayed Messenger RNAs Are Translated and Lead to Enhanced

Protein Expression.

Through the use of β-Galactosidase-specific antibodies, results show increased

protein content in cell cultures (of comparable cell concentrations as measured by optical

density) containing the decay-resistant structures (FIGURE 12). As seen in Figure 12, the

most prominent band is observed at the correct molecular weight (116 kD) for β-

Galactosidase only for cells containing the Xrn1-resistant structures.

The β-Galactosidase Assay also revealed increased enzymatic activity of the cells

expressing the reporters containing the fully-functioning xrRNAs and IRES elements.

After normalization by time and cell concentration (absorbance at 600 nm), as well as

subtracting the enzymatic activity in wild-type cells, addition of Xrn1-resistant structures

resulted in approximately 32-fold increase in enzymatic activity (FIGURE 13, TABLE

S1). Results from the enzymatic activity assay and western blot demonstrate that the

partially-decayed messenger RNAs are successfully translated in the H2545 cells.

3.5   DXO1 knockouts display increased enzymatic activity after transformation with
JPS 1480s series reporters

CRY1 cells (W303-1A) wild-type cells, as well as knockouts for *XRN1, DXO1,*

and *XRN1/DXO1* were transformed with the JPS 1480 series reporters 1481, 1481X, and

1481M. CRY1 cells contain all four *IMT* genes, suggesting that cap-dependent translation

in these cells should be favored and internal-ribosomal entry should not be observed. β-

galactosidase assay was performed on all resulting cells, and the results indicated that

cap-independent translation of the IRES is active in the *DXO1* knockout strain, as shown

by the increased enzymatic activity of β-galactosidase in the cells expressing the

functioning xrRNAs (FIGURE 14). The *DXO1* knockout expressing the JPS 1481X

reporter was calculated to have an enzymatic activity corresponding to 96.7 Miller Units,

a significant increase compared to the 1.2 Miller Units calculated for the WT strain

expressing the same reporter (FIGURE 14), and the 1.4 Miller Units calculated for the

empty Δ*DXO1* cells (FIGURE S3).
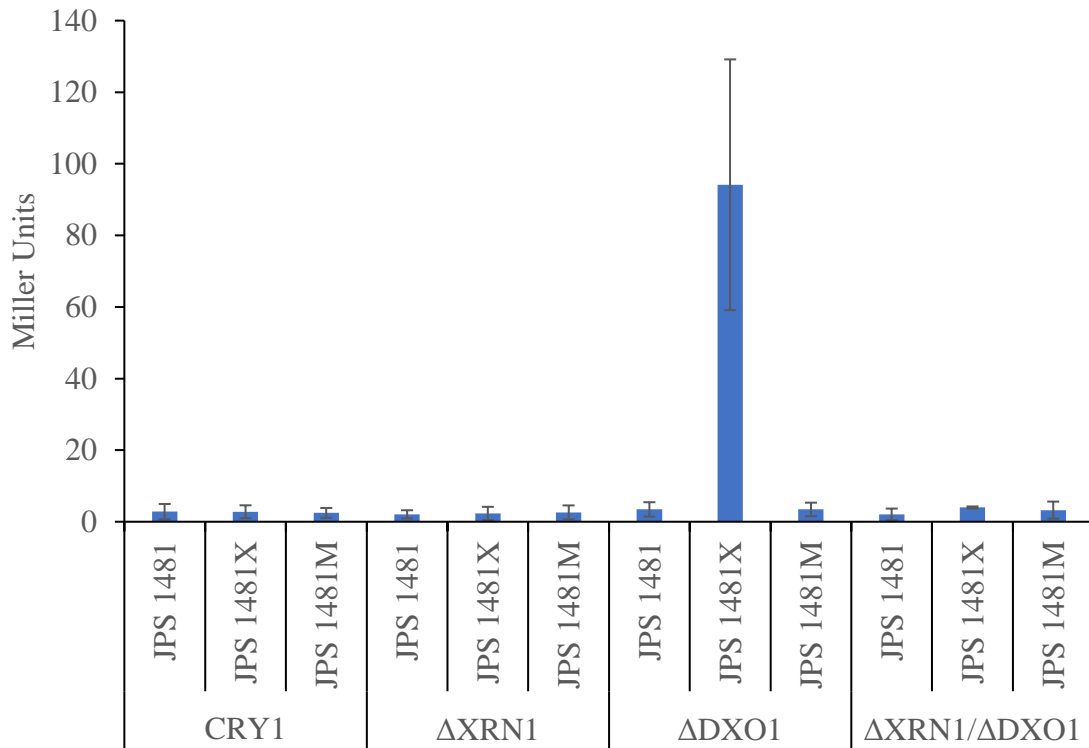
FIGURE 14. β-galactosidase activity of WT CRY1 cells and three different knockout strains expressing three of the reporters from the JPS 1480 series. Total yeast protein lysates were incubated with ONPG for 3 hours. Enzymatic activity was quantified as absorbance at 420 nm and normalized for reaction time and initial cell concentration, measured as absorbance at 600 nm. β-galactosidase activity of WT CRY1 cells and three different knockout strains expressing three of the reporters from the JPS 1480 series. The increased enzymatic activity observed in the *DXO1* knockout strain suggests that cap-independent translation of the CrPV IRES element is active in this strain.

Surprisingly, the double-knockout cells (ΔXRN1/ΔDXO1) did not exhibit increased β-galactosidase activity. In order to genetically rescue the double-knockout strain, cells were transformed with plasmids containing the full XRN1 ORF. Two different plasmids were used. The first was a commercial yeast ORF, obtained from

Dharmacon and containing a (-ura) selective marker (Dharmacon product # YSC3869-

202330614). The second plasmid was a gift from Jay R. Hesselberth's lab and contains a

(-leu) selective marker (Plasmid BJH 872). Both sets of cells were tested via β-

galactosidase assay but did not demonstrate any increased enzymatic activity compared

to the empty cells (Figure S3). These results indicate that adding the XRN1 ORF to the

ΔXRN1/ΔDXO1 strain does not genetically rescue IRES activity in this strain.
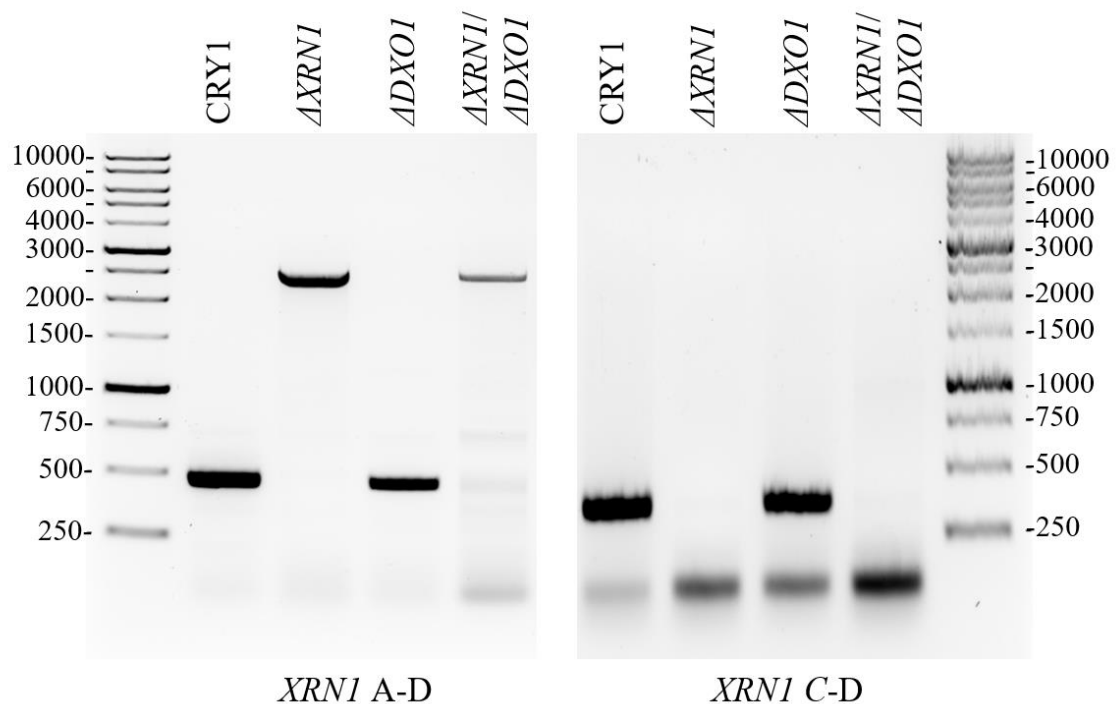
FIGURE 15. Colony PCR confirmation of Δ*XRN1* genotype (*xrn1Δ::HygMX*). Large individual colonies of wild-type CRY1 cells, as well as knockouts for *XRN1, DXO1* and *XRN1/DXO1,* were resuspended in lysis buffer and lysed by heating to 95 °C. Lysates were used as templates for PCR amplification using *XRN1*-specific primers and subjected to equal reaction conditions. PCR products were analyzed through gel electrophoresis. The PCR product obtained at around 2200 bp (left) in the Δ*XRN1* and Δ*XRN1*/Δ*DXO1* strains confirms that, in these cells, the *XRN1* ORF has been replaced with the *HygMX* cassette, yielding the knockout genotype. The PCR product observed at around 460 bp in the CRY1 (and Δ*DXO1*) cells confirms that the wild-type cells contain the *XRN1* ORF.

Since genetic rescue of the *XRN1/DXO1* knockout strain was unsuccessful, it was important to confirm the genotype of the cells, as well as the sequence of the pXRN1 plasmid. All four strains were subjected to colony PCR analysis using the target specific primers listed in TABLE 2.
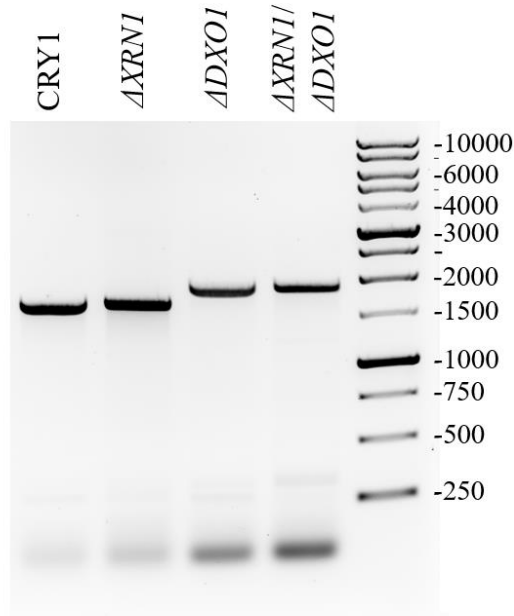
DXO1 A-D

FIGURE 16. Colony PCR confirmation of the Δ*DXO1* genotype (*dxo1Δ::KanMX*). Large individual colonies of wild-type CRY1 cells, as well as knockouts for *XRN1, DXO1* and *XRN1/DXO1,* were resuspended in lysis buffer and lysed by heating to 95 °C. Lysates were used as templates for PCR amplification using *DXO1*-specific primers, subjected to equal reaction conditions, and analyzed through gel electrophoresis. The results confirm the WT and mutant genotype, as observed in the difference in length between the PCR products observed at around 1980 bp in the CRY1 (and Δ*XRN1*) cells and the products observed at around 2000 bp in the two Δ*DXO1* strains.

Results from the colony PCR experiments confirm that the *XRN1* gene is not present in the Δ*XRN1* and Δ*XRN1*/Δ*DXO1* strains, but is present in the WT CRY1 strain

48

and the ΔDXO1 strain (FIGURE 15). Primers A and D (left) land in the adjacent regions of the genome to the *XRN1* gene and should yield PCR products corresponding to either the full *XRN1* ORF (plus flanking regions) in the WT cells or the *HygMX* cassette in the knockout cells. The full-length product for the WT cells, expected at a length of 5213 bp, was not observed. The resulting PCR product observed in the knockout cells, at around 2202 bp, corresponds to the expected length and serves as confirmation of the genotype of the ΔXRN1cells. The genotype of the WT cells was confirmed by using primer C (right), which lands inside the ORF and should therefore only yield a PCR product (460 bp) in cells that contain the *XRN1* ORF.

Similarly, by using primers that land in the flanking regions of the genome to the *DXO1* ORF, the difference in lengths between the WT and knockout strains can be observed (FIGURE 16). The CRY1 and ΔXRN1 contain the full *DXO1* ORF, and therefore yield PCR products observed at around 1980 bp. In the knockout strains, the *DXO1* ORF has been replaced with the *KanMX* cassette, which is slightly longer, resulting in the observed bands at around 2008 bp in the ΔDXO1 and the ΔXRN1/ΔDXO1 strains.

Sequencing results of the BJH 872 plasmid encoding for pXRN1 should confirm that the plasmid encodes for the full-length protein, which should be fully-functioning (FIGURE S4, pending last sequencing results). The fact that the ΔXRN1/ΔDXO1 cells that were transformed with both the BJH 872 plasmid and the JPS 1480 series plasmids (either 1481, 1481X, or 1481M) were capable of growing in SD media lacking both uracil and leucine suggests that the cells were expressing both plasmids simultaneously.

Since the sequencing results of the BJH 872 plasmid suggest that the plasmid does encode the full-length protein, the failure to genetically rescue the double-knockout mutant to behave similarly to the Δ*DXO1* mutant is surprising.

CHAPTER FOUR: DISCUSSION AND SUMMARY

Xrn1 is the major eukaryotic exonuclease and binds to a 5' monophosphate substrate exposed after removal of the m^7G cap by a decapping enzyme (Dcp1 in yeast). Xrn1 proceeds in the 5'→3' direction but can be effectively stopped by the pseudoknot structures encoded in the 3'UTR of the genome of Flaviviruses (Chapman et al., 2014). These Xrn1-resistant structures, named xrRNAs, have potential therapeutic and industrial applications, since they can theoretically be used to enhance protein expression of target genes by protecting them from degradation. Current usage of recombinant DNA technology includes a wide-range of applications in which target proteins and metabolites are produced at a large scale in order to improve human health and lifestyle (Khan et al., 2016). These applications include synthesis of vaccines (Zhang et al., 2011), pharmaceuticals (Lomedico, 1982), biofuels (Ullah et al., 2015), alternative energy sources (Tiwari and Pandey, 2012), and could have promising uses in the development of mRNA therapeutics (Zhong et al., 2018). Using a combination of existing recombinant DNA technology with xrRNAs can substantially increase the effectiveness of these and many other applications.

Our results support the hypothesis that artificially-installed Xrn1-resistant structures protect RNA transcripts and lead to increased expression of downstream genes (FIGURES 12, 13, 14, S3). The β-galactosidase assay indicates an average 32-fold increase in enzymatic activity in cells expressing the decay-resistant structures, compared to cells expressing the reporter without the decay-resistant structures (FIGURE 13, TABLE S1). Interestingly, there is a small increase in enzymatic activity (1.25x) found with the cells expressing the mutant version of the decay-resistant structures, suggesting the mutant structures provide a small level of protection from degradation. This effect is consistently observed and should be investigated. The IRES-dead mutants (1482 and 1482X) do not appear to exhibit any increase in enzymatic activity, providing evidence that the IRES is indeed inactive and cap-independent translation does not occur. Future directions can include analysis of analogous reporters containing a galactose-inducible reporter. This should allow for quantification of protein expression over time in order to compare the difference in the rate of mRNA decay

Fragment analysis results showed the build-up of xrRNA-protected transcripts containing one and two copies of the viral pseudoknot structure (FIGURE 11). Future directions can include detection of the longer RNA transcripts (above 500-600 bp), as well as analysis of the IRES-dead mutants (1482 and 1482X). Since the IRES-dead mutants contained fully-functioning Xrn1-resistant structures, the length of the transcripts detected should be identical to those found in the IRES-active reporters. This should provide evidence that, even in the presence of fully-active Xrn1-resistant structures (and

therefore an increased concentration of transcripts), increased protein expression is not possible without also a fully active IRES.

H2545 *S. cerevisiae* cells are ideal for the investigation of reporters including the CrPV IRES, since they contain genetic mutations that have been shown to be conducive to successful cap-independent translation via internal-ribosomal entry (Thompson et al., 2001). Our results confirm that IRES-dependent translation is active in these cells (FIGURE 13). Our results also show that the two artificially-installed viral structures (xrRNAs and CrPV IRES) work in tandem, since the reporters were successfully transcribed and translated (FIGURES 11 and 13).

In order to examine the effect of the deletion of genes *XRN1* and *DXO1* in the rate of cap-independent translation, a different strain was used, whose wild-type cells were expected to show no IRES activity. β-galactosidase assay results of the empty wild-type CRY1 cells, as well as the empty knockout cells, served as a control and established the basal level of enzymatic activity in this strain (FIGURE S3). As expected, after transformation with the JPS 1481X reporter, the wild-type CRY1 cells did not show increased enzymatic activity when compared to the empty cells, confirming that the CrPV structure encoded in the reporter does not successfully initiate translation in the wild-type cells. However, when the *DXO1* gene is deleted, we saw an average 64-fold increase in enzymatic activity (FIGURE S3, 96.7 Miller units) in the cells expressing the JPS 1481X reporter when compared to the empty cells (1.2 Miller units in CRY1 cells and 1.4 Miller units in *DXO1*). Therefore, our results show that deletion of *DXO1* changes cellular conditions enough to allow for successful IRES-dependent translation.

Thompson et al. reported that the CrPV IRES functioned successfully in cells that had lower cellular concentrations of the eIF2•GTP•Met–tRNA$_i^{Met}$ ternary complex, either due to the disruption of two initiator tRNA^{Met} genes (cells used in this work), or due to constitutive expression of the eIF2 kinase GCN2. Our results indicate that deletion of *DXO1* also leads to decreased concentrations of the eIF2•GTP•Met–tRNA$_i^{Met}$ ternary complex.

DXO1 is a predominantly cytoplasmic decapping exonuclease found in some yeast. This enzyme is involved in mRNA 5'-end-capping quality-control and has 5'→3' exonuclease activity. It has 5' triophosphonucleotide hydrolase activity and preferentially decaps transcripts with unmethylated caps. Its exonuclease activity allows it to single-handedly decap and degrade faulty mRNAs (Chang et al., 2012). Based on current knowledge, disruption of either the decapping or the exonuclease activity of DXO1 should not decrease the cellular concentration of the eIF2•GTP•Met–tRNA$_i^{Met}$ ternary complex. It remains unclear how deletion of the *DXO1* gene leads to the ability of the knockout cells to successfully initiate translation using the CrPV IRES. Since our results suggest that deletion of the *DXO1* gene makes cap-dependent translation less favorable, and since it has been shown that DXO1 interacts with the 5' end of an mRNA, it is possible that this enzyme plays an additional role in the cell and is somehow involved in formation of the translation pre-initiation complex.

REFERENCES

Acker, M.G. et al. Kinetic analysis of late steps of eukaryotic translation initiation. *J. Mol. Biol*. **2009**, 385, 491–506.

Aiktek, C. E.; Lorsch, J. R. A mechanistic overview of translation initiation in eukaryotes. *Nat. Struct. Mol. Biol.* **2012**, 19 (6), 568-576. DOI:10.1038/nsmb.2303.

Akiyama, B. J.; Laurence, H. M.' Massey, A. R.; Constantino, D. A.; Xie, X.; Yang, Y.; Shi, P. Y.; Nix, J. C.; Beckham, J. D.; Kieft, J. S. Zika virus produces noncoding RNAs using a multi-pseudoknot structure that confounds a cellular exonuclease. *Science*. **2016**, 354 (6316), 1148-1152.

Algire, M. A.; et al. Development and characterization of a reconstituted yeast translation initiation system. *RNA*. **2002**, 8, 382-397.

Alonso, C. R. A complex 'mRNA degradation code' controls gene expression during animal development. *Trends Genet.* **2012**, 28 (2), 78-88.

Bakhshesh, M.; Groppelli, E.; Willcocks, M. M.; Royall, E.; Belsham, G.J.; Roberts, L.O. The picornavirus avian encephalomyelitis virus possesses a hepatitis C virus-like internal ribosome entry site element. *J. Virol.* **2008**, 82, 1993-2003.

Beelman, C. A.; Parker, R. Degradation of mRNA in eukaryotes. *Cell*. **1995**, 81, 179-183.

Billard, S.; Lopez-Villavicencio, M.; Hood, M. W.; Gud, T. Sex, outcrossing and mating types: unsolved questions in fungi and beyond. *J. Evol. Biol*. **2012**, 25 (6), 1020-1038. DOI: 10.1111/j.1420-9101.2012.02495.x

Borman, A.; Jackson, R.J. Initiation of translation of human rhinovirus RNA: mapping the internal ribosome entry site. *Virology*. **1992**, 188, 685-696.

Brickner, J. H.; Fuller, R. S. SOI1 encodes a novel, conserved protein that promotes TGN-endosomal cycling of Kex2p and other membrane proteins by modulating the function of two TGN localization signals. *J. Cell. Biol.* **1997**, 139 (1), 23-36.

Brown, E. A.; Day, S.P.; Jansen, R.W.; Lemon, S.M. The 5′ nontranslated region of hepatitis A virus RNA: secondary structure and elements required for translation in vitro. *J. Virol*. **1991**, 65, 5828-5838.

Byström, A. S.; Fink, G. R. A functional analysis of the repeated methionine initiator tRNA genes (*IMT*) in yeast. *Mol. Gen. Genet.* **1989**, 216, 276-286.

Caponigro, G.; Parker, R. Mechanisms and control of mRNA turnover in Saccharomyces cerevisiae. *Microbiol. Rev*. **1996**, 60, 233–249.

Chang, J. H.; Jiao, X.; Chiba, K.; Oh, C.; Martin, C. E.; Kiledjian, M.; Tong, L. Dxo1 is a new type of eukaryotic enzyme with both decapping and 5'-3' exoribonuclease activity. *Nat Struct Mol Biol.* **2012**, 19 (10), 1011-7. doi: 10.1038/nsmb.2381.

Chapman, E. G.; Constantino, D. A.; Rabe, J. L.; Moon, S. L.; Wilusz, J.; Nix, J. C.; Kieft, J. S. The structural basis of pathogenic subgenomic flavivirus RNA (sfRNA) production. *Science.* **2014**, 344 (6181), 307-310.

Chapman, E. G.; Moon, S. L.; Wilusz, J.; Kieft, J. S. RNA Structures that resist degradation by xrn1 produce a pathogenic dengue virus RNA. Ed. Timothy Nilsen. *eLife*. **2014**, 3:e01892. DOI: 10.7554/eLife.01892.

Cherry, J. M. Genetic nomenclature guide. *Trends Genet.* 1998, 11-2. PMID: 7660459.

Cherry, P. D.; Peach, S.; Hesselberth, J. R. Multiple decay events target HAC1 mRNA during splicing to regulate the unfolded protein response. *eLife* **2019**, 8:e42262. DOI: 10.7554/eLife.42262

Chu A. M.; Davis, R. W. High-throughput creation of a whole-genome collection of yeast knockout strains. *Methods Mol. Biol.* (Clifton, N.J.). **2008**, 416, 205-20 PMID:18392970

Decker, C. J.; Parker, R. A turnover pathway for both stable and unstable mRNAs in yeast: evidence for a requirement for deadenylation. *Genes Dev.* **1993**, 7, 1632-1643.

Dever, T. E.; Yang, W.; Åström, A. S.; Byström, A. S.; Hinnebusch, A. G. Modulation of tRNA$_i^{Met}$, eIF-2, and eIF-2B expression shows that *GCN4* translation is inversely coupled to the level of eIF-2•GTP•Met-tRNA$_i^{Met}$ Ternary Complexes. *Mol. Cell. Biol.* **1995**, 15 (11), 6351-6363.

Domier, L. L.; McCoppin, N. K.; D'Arcy, C. J. Sequence requirements for translation initiation of Rhopalosiphum padi virus ORF2. *Virology.* **2000**, 268, 264–271.

Dourfman, B. Z. The isolation of adenylosuccinate synthetase mutants in yeast by selection for constitutive behavior in pigmented strains. *Genetics.* **1969**, 61 (2), 377-89

Douglas, H. C.; Condie, F. The genetic control of galactose utilization in Saccharomyces. *J. Bacteriol.* **1954**, 68 (6), 662-670.

Douglas, H. C.; Hawthorne, D. C. Enzymatic expression and genetic linkage of genes controlling galactose utilization in Saccharomyces. *Genetics.* **1964**, 49 (5), 837-844.

Duina, A. A.; Miller, M. E.; Keeney, J. B. Budding yeast for budding geneticists: a primer on the saccharomyces cerevisiae model system. *Genetics*. **2014**, 197 (1), 33-48.

Eraslan, B.; Wang, D. X.; Gusic, M.; Prokisch, H.; Hallstrom, B. M.; Uhlen, M.; Asplund, A.; Ponten, F.; Wieland, T.; Hopf, T.; Hahne, H.; Kuster, B.; Gagneur, J. Quantification and discovery of sequence determinants of protein-per-mRNA amount in 29 human tissues. *Mol. Syst. Biol.* **2019**, 15 (2), e8513. DOI: 10.15252/msb.20188513

Flynn, P. J.; Reece, R. J. Activation of transcription by metabolic intermediates of the pyrimidine biosynthetic pathway. *Mol. Cell. Biol.* **1999**, 19 (1), 882–888. doi:10.1128/mcb.19.1.882

Frolova, L.; Le Goff, X.; Rasmussen, H. H.; Cheperegin, S.; Drugeon, G.; Kress, M.; Arman, I.; Haenni, A. L.; Celis, J. E.; Philippe, M. A highly conserved eukaryotic

protein family possessing properties of polypeptide chain release factor. *Nature*. **1994**, 372 (6507): 701–3. doi:10.1038/372701a0.

Garneau, N. L.; Wilusz, J.; Wilusz, C. J. The highways and byways of mRNA decay. *Nat. Rev. Mol. Cell Biol.* **2007**, 8, 113-126.

Geerlings, T. H. et al. The final step in the formation of 25S rRNA in Saccharomyces cerevisiae is performed by 5'-->3' exonucleases. *RNA*. **2000**, 6 (12), 1698-1703.

Glover-Cutter, K.; Kim, S.; Espinosa, J.; Bentley, D. L. RNA polymerase II pauses and associates with pre-mRNA processing factors at both ends of genes. *Nat. Struct. Mol. Biol.* **2008**, 15 (1), 71-78.

Goffeau A.; Barrell, B.G.; Bussey, H.; Davis, R. W.; Dujon, B.; Feldmann, H.; Galibert, F.; Hoheisel, J. D.; Jacq, C.; Johnston, M.; Louis, E. J.; Mewes, H. W.; Murakami, Y.; Philippsen, P.; Tettelin, H.; Oliver, S. G.. Life with 6000 genes. *Science*. **1996**, 274 (5287), 546-567.

Gounatopoulos-Pournatzis, T.; Cowling, V. H. Cap-binding complex (CBC). *Biochem J.* **2013**, 457 (Pt 2), 231-242.

Hamm, J.; Mattaj, I. W. Monomethylated cap structures facilitate RNA export from the nucleus. *Cell*. **1990**, 63 (1), 109-118.

Hellen, C. U. T. Translation Termination and ribosome recycling in eukaryotes. *Cold Spring Harb. Perspect. Biol.* **2018**. DOI: 10.1101/cshperspect.a032656

Hellen, C. U. T.; Sarnow, P. Internal ribosome entry sites in eukaryotic mRNA molecules. *Genes Dev.* **2019**, 15, 1593-1612.

Hinnebusch, A. G. Molecular mechanism of scanning and start codon selection in eukaryotes. *Microbiol. Mol. Biol. Rev*. 2011, 75, 434–467.

Hinton, T.M.; Crabb, B.S. The novel picornavirus Equine rhinitis B virus contains a strong type II internal ribosomal entry site which functions similarly to that of Encephalomyocarditis virus**.** *J. Gen. Virol*. **2001**, 82, 2257-2269

Hsu, C. L.; Stevens, A. Yeast cells lacking 5' to 3' exoribonuclease 1 contain mRNA species that are poly(A) deficient and partially lack the 5' cap structure. *Mol. Cell. Biol*. **1993**, 13, 4826-4835.

Jackson, R. J.; Howell, M. T.; Kamisnki, A. The novel mechanism of initiation of picornavirus RNA translation. Trends Biochem. Sci. 1990, 15 (12), 477-483.

Jacobson, A. Poly(A) metabolism and translation: the closed-loop model. In Hershey, J.W.B.; Mathews, M.B.; Sonenberg, N. (eds), Translational Control. Cold Spring Harbor Laboratory Press, Cold Spring Harbor. **1996**, NY, pp. 451–480.

Jang, S.K., Krausslich, H.G., Nicklin, M.J., Duke, G.M., Palmenberg, A.C., and Wimmer, E. A segment of the 5' nontranslated region of encephalomyocarditis virus RNA directs internal entry of ribosomes during in vitro translation. *J. Virol*. **1988**, 62, 2636–2643.

Jones, C. I.; Zabolotskaya, M. V.; Newbury, S. F. The 5′ → 3′ exoribonuclease XRN1/Pacman and its functions in cellular processes and development. *Wiley Interdiscip. Rev. RNA*. **2012**, 3, 455–468. doi:10.1002/wrna.1109 pmid:22383165.

Kahvejian, A.; Roy, G.; Sonenberg, N. The mRNA closed-loop model: The function of PABP and PABP-interacting proteins in mRNA translation. *Cold Spring Harbor Symp. Quant. Biol*. **2001**, 66, 293-300.

Kanamori, Y.; Nakashima, N. A tertiary structure model of the internal ribosome entry site (IRES) for methionine-independent initiation of translation. *RNA*. **2001**, 7, 266–274.

Khan, S.; Ullah, M. W.; Siddique, R.; Nabi, G.; Manan, S.; Yousaf, M.; Hou, H. Role of recombinant dna technology to improve life. *Int. J. Genomics*. **2016**, 2405954. doi:10.1155/2016/2405954

Konarska, M.; Filipowicz, W.; Domdey, H.; Gross, H.J. Binding of ribosomes to linear and circular forms of the 5'- terminal leader fragment of tobacco-mosaic-virus RNA. *Eur. J. Biochem*. **1981**, 114, 221–227

Kosark, M. Inability of circular mRNA to attach to eukaryotic ribosomes. *Nature*. **1979**, 28, 82-85.

Kramer, A. The structure and function of proteins involved in mammalian pre-mRNA splicing. *Annu. Rev. Biochem.* **1996**, 65, 367-409.

Kushnirov, V. V. Rapid and reliable protein extraction from yeast. *Yeast*. **2000**, 16 (9), 857-860. Doi: 10.1002/1097-0061(20000630)16:9<857::AID-YEA561>3.0.CO;2-B.

LaGrandeur, T. E.; Parker, R. Isolation and characterization of Dcp1p, the yeast mRNA decapping enzyme. *EMBO J*. **1998**, 17 (5), 1487-96.

Liu, Y.; Liu, H.; Zou, J.; Zhang, B.; Yuan, Z. Dengue virus subgenomic RNA induces apoptosis through the Bcl-2-mediated PI3k/Akt signaling pathway. *Virology*. **2014**, 448, 15–25.

Lomedico P. T. Use of recombinant DNA technology to program eukaryotic cells to synthesize rat proinsulin: a rapid expression assay for cloned genes. *Proc. Natl. Acad. Sci. U. S. A*. **1982**, 79 (19), 5798–5802. doi: 10.1073/pnas.79.19.5798.

Maag, D.; Fekete, C., Gryczynski, Z.; Lorsch, J. A conformational change in the eukaryotic translation preinitiation complex and release of eIF1 signal recognition of the start codon. *Mol. Cell*. **2005**, 17, 265–275.

Martinez-Salas, E.; Francisco-Velilla, R.; Fernandez-Chamorro, J.; Lozano, G.; Diaz-Toledano, R. Picornavirus IRES elements: RNA structure and host protein interactions. *Virus Res.* **2015**, 206, 62-73.

Mayas, R. M.; Maita, H.; Semlow, D. R.; Staley, J. P. Spliceosome discards intermediates via the DEAH Box ATPase Prp43p. *PNAS*. **2010**, 107 (22), 10020–10025. PMC. Web. 2 Mar. 2018.Sdf.

Merrick, W. C. Mechanism and regulation of eukaryotic protein synthesis. *Microbiol. Rev*. **1992**, 56 (2), 291-315.

Miller J. H. Experiments in molecular genetics, Cold Spring Harbor Laboratory Press Cold Spring Harbor; NY: 1972.

Mitchell, P.; Tollervey, D. An NMD pathway in yeast involving accelerated deadenylation and exosome-mediated 3 '-> 5 ' degradation. *Molecular Cell,* **2003**, 11 (5), 1405-1413.

Moore, M. J.; Sharp, P. A. Evidence for two active sites in the spliceosome provided by stereochemistry of pre-mRNA splicing. *Nature*. **1993**, 365, 364-368.

Mortimer, R. K; Johnston, J. R. Genealogy of principal strains of the yeast genetic stock center. *Genetics*. **1986**, 113 (1), 35-43. PMID:3519363

Muhlrad, D.; Decker, C. J.; Parker, R. Deadenylation of the unstable mRNA encoded by the yeast MFA2 gene leads to decapping followed by 5' 3' digestion of the transcript. *Genes Dev*. **1994**, 8(7), 855-866.

Muhlrad, D.; Parker, R. Mutations affecting stability and deadenylation of the yeast MFA2 transcript. *Genes Dev.* **1992**, 6(11), 2100-2111.

Orphanides, G.; Lagrange, T.; Reinberg, D. The general transcription factors of RNA polymerase II. *Genes & Dev.* **1996**, 10, 2657-2683.

Pain, V. M. Initiation of protein synthesis in eukaryotic cells. *Eur. J. Biochem.* **1996,** 236, 747–771

Parker, R. RNA Degradation in *Saccharomyces cerevisae*. *Genetics*. **2012**, 191 (3), 671-702.

Pavitt, G. D.; Proud, C. G. Protein synthesis and its control in neuronal cells with a focus on vanishing white matter disease. *Biochem. Soc. Trans*. **2009**, 37 (6), 1298-1310.

Pelletier, J.; Sonenberg, N. Internal initiation of translation of eukaryotic mRNA directed by a sequence derived from poliovirus RNA. *Nature*. **1988**, 334: 320–325

Pestova, T.V.; Shatsky, I.N.; Fletcher, S.P.; Jackson, R.J.; Hellen, C.U. A prokaryotic-like mode of cytoplasmic eukaryotic ribosome binding to the initiation codon during internal translation initiation of hepatitis C and classical swine fever virus RNAs. *Genes & Dev*. **1998**, 12, 67–83.

Pestova, T.V. et al. The joining of ribosomal subunits in eukaryotes requires eIF5B. *Nature.* **2000,** 403, 332–335.

Pijlman, G. P.; Funk, A.; Kondratieva, N.; Leung, J.; Torres, S.; Van Der Aa, L.; Liu, W. J.; Palmenberg, A. C.; Shi, P. Y.; Hall, R. A.; Khromykh, A. A. A highly structured, nuclease-resistant, noncoding RNA produced by flaviviruses is required for pathogenicity. *Cell Host Microbe*. **2008**, 4 (6), 579–591.

Pisareva, V. P.; Pisarev, A. V.; Fernandez, I. S. Dual tRNA mimicry in the Cricket Paralysis Virus IRES uncovers an unexpected similarity with the Hepatitis C Virus IRES. *eLife*. **2018**, 7:e34062. DOI: https://doi.org/10.7554/eLife.34062

Proudfoot, N. J.; Furger, A.; Dye, M. J. Integrating mRNA processing with transcription. *Cell*. **2002**, 108 (4), 501-512.

Rocak, S.; Linder, P. DEAD-box proteins: the driving forces behind RNA metabolism. *Nat Rev Mol Cell Biol*, **2004**, 5, 232-24

Rose, M.; Winston, F. Identification of a Ty insertion within the coding sequence of the S. cerevisiae *URA3* gene. *Mol. Gen. Genet*. **1984**, 193 (3), 557-560.

Ross, J. mRNA stability in Mammalian Cells. *Microbiol. Rev*. **1995**, 59 (3), 423-450.

Sachs, A. B.; Sarnow, P.; Hentze, M. W. Starting at the beginning, middle, and end: translation initiation in eukaryotes. *Cell*. **1997**, 89, 831-838.

Sasaki, J.; Nakashima, N. Translation initiation at the CUU codon is mediated by the internal ribosome entry site of an insect picorna-like virus in vitro. *J. Virol.* **1999**, 73, 1219–1226.

Sato, H.; Maquat, L. E. Remodeling of the pioneer translation initiation complex involves translation and the karyopherin importin β. *Genes Dev.* **2009**, 23, 2537-2550.

Scheiness, D.; Damell, J. E. Polyadenylic acid segment in mRNA becomes shorter with age. *Nature New Biol*. **1973**, 241, 265-268.

Schüler, M.; Connell, S.; Lescoute, A.; Giesebrecht, J.; Dabrowski, M.; Schroeer, B.; Mielke, T.; Penczek, P.; Westhof, E.; Spahn, C. M. T. Structure of the ribosome-bound cricket paralysis virus IRES RNA. *Nat. Struct. Mol. Biol.* **2007**, 13 (12), 1092-1096.

Sharova, L. V.; Alexei, A. S.; Nedorezov, T.; Piao, Y.; Nabeebi, S.; Ko, M. S. Database for mRNA half-life of 19 977 genes obtained by DNA microarray analysis of pluripotent and differentiating mouse embryonic stem cells. *DNA Res.* **2008**, 16 (1), 45-58.

Shoemake, D. D.; Lashkari, D. A.; Morris, D.; Mittmann, M.; Davis, R. W. Quantitative phenotypic analysis of yeast deletion mutants using a highly parallel molecular bar-coding strategy. *Nat Genet*. **1996**, 14(4), 450-6.

Sonenberg, N. mRNA 5 cap-binding protein eIF4E and control of cell growth. In Hershey, J.W.B.; Mathews, M.B.; Sonenberg, N. (eds), Translational control. Cold Spring Harbor Laboratory Press, Cold Spring Harbor, NY, **1996** pp. 271–294.

Sonenberg, N.; Dever, T. E. Eukaryotic translation initiation factors and regulators. *Curr Opin Cell Biol.* **2006**, 18 (3), 299-306.

Tarun, S. Z.; Sachs, A. B. Association of the yeast poly(A) tail binding protein with translation initiation factor eIF4G. *EMBO J*. **1996**, 15, 7168–7177.

Thompson S. R.; Gulyas K. D.; Sarnow P. Internal initiation in Saccharomyces cerevisiae mediated by an initiator tRNA/eIF2-independent internal ribosome entry site element. *PNAS*. 2001, 98 (23), 12972-12977.

Tiwari, A.; Pandey, A. Cyanobacterial hydrogen production—a step towards clean environment. *Int. J. Hydrogen Energy*. **2012**, 37 (1), 139–150. doi:10.1016/j.ijhydene.2011.09.100.

Ullah, M. W.; Khattak, W. A.; Ul-Islam, M.; Khan, S.; Park J. K. Encapsulated yeast cell-free system: a strategy for cost-effective and sustainable production of bio-ethanol in consecutive batches. *Biotechnol. Bioprocess Eng*. **2015**, 20 (3), 561–575. doi: 10.1007/s12257-014-0855-1.

Vihervaara, A.; Duarte, F. M.; Lis, J. T. Molecular mechanisms driving transcriptional stress responses. *Nature*. **2018**, 19, 385-397.

Wahle, E.; Ruegsegger, U. 3'-End processing of pre-mRNA in eukaryotes. *FEMS Microbiology Reviews*. **1999**, 23, 277-295.

Weiss, I. M.; Liebhaber, S. A. Erythroid specific determinants of a-globin mRNA stability. *Mol. Cell. Biol*. **1994**, 14, 8123–8132.

Westaway, E. G.; Brinton, M. A.; Gaidamovich, S.; Horzinek, M. C.; Igarashi, A.; Kaariainen, L.; Lvov, D. K.; Porterfield, J. S.; Russell, P. K.; Trent, D. W. Flaviviridae. *Intervirology*. **1985**, 24, 183–192.

Wilson, J. E.; Pestova, T.V.; Hellen, C.U.; Sarnow, P. Initiation of protein synthesis from the A site of the ribosome. *Cell*. **2000**, 102, 511–520.

Wilson, J. E.; Powell, M. J.; Hoover, S. E.; Sarnow, P. Naturally occurring dicistronic cricket paralysis virus RNA is regulated by two internal ribosome entry sites. *Mol. Cell. Biol*. **2000**, 20, 4990–4999.

Zhang J.; Tarbet E. B.; Toro H.; Tang D.-C. C. Adenovirus-vectored drug-vaccine duo as a potential driver for conferring mass protection against infectious diseases. *Expert Rev. Vaccines*. **2011**, 10 (11), 1539–1552. doi: 10.1586/erv.11.141.

Zhong, Z.; Mc Cafferty, S.; Combes, F.; Huysmans, H.; De Temmerman, J.; Gitsels, A.; Vanrompay, D.; Portena Catani, J.; Sanders, N. N. mRNA therapeutics deliver a hopeful message. *NanoToday*. **2018**, 23, 16-39,

APPENDIX A

SUPPLEMENTAL INFORMATION

FIGURE S1. Comprehensive map of reporter vectors JPS 1481 (top) and 1481X (bottom), containing all key features, restriction enzyme cleavage sites, and primers used for sequencing (shown by lime green arrows indicating direction of primer). New LacZ PE primer was also used for reverse transcription.

	Miller units					
	30-Aug	31-Aug	8-Sept (1)	8-Sept (2)	Mean	St Dev
JPS 1481	4.37	6.55	3.20	3.03	4	2
JPS 1481 X	124.33	155.67	102.00	128.66	128	22
JPS 1481 M	3.95	6.56	4.57	5.10	5	1
JPS 1482	3.05	6.07	2.31	2.89	4	2
JPS 1482 X	2.60	4.11	1.17	2.06	2	1

TABLE S1. Quantitative results of β-galactosidase assay of H2545 cells expressing different JPS 1480 series reporters. Total yeast protein lysates were incubated with ONPG for 3 hours. Enzymatic activity was quantified as absorbance at 420 nm and normalized for reaction time and initial cell concentration, measured as absorbance at 600 nm.
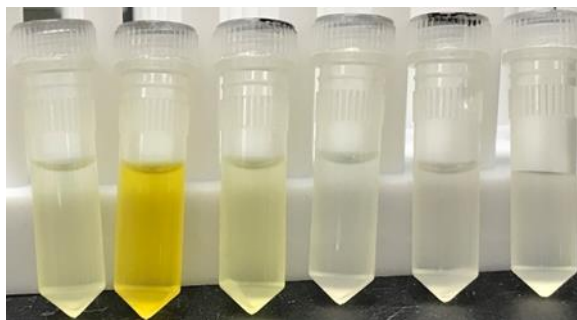
FIGURE S2. Qualitative results of β-galactosidase assay of H2545 cells expressing different. The tubes, listed from left-to-right, belong to cells expressing the following JPS 1480 series reporters: 1481, 1481X, 1481M, 1482, 1482X, and empty cells. As results indicate, cells containing the IRES-dead elements have close to the same enzymatic activity as the empty cells (1482, 1482X). The cells containing the functioning IRES but inactive xrRNAs have some increased activity, as evidenced by the light yellow color (1481, 1481M). The cells with the highest activity are those in which both elements are active (1481X, second tube from the left).
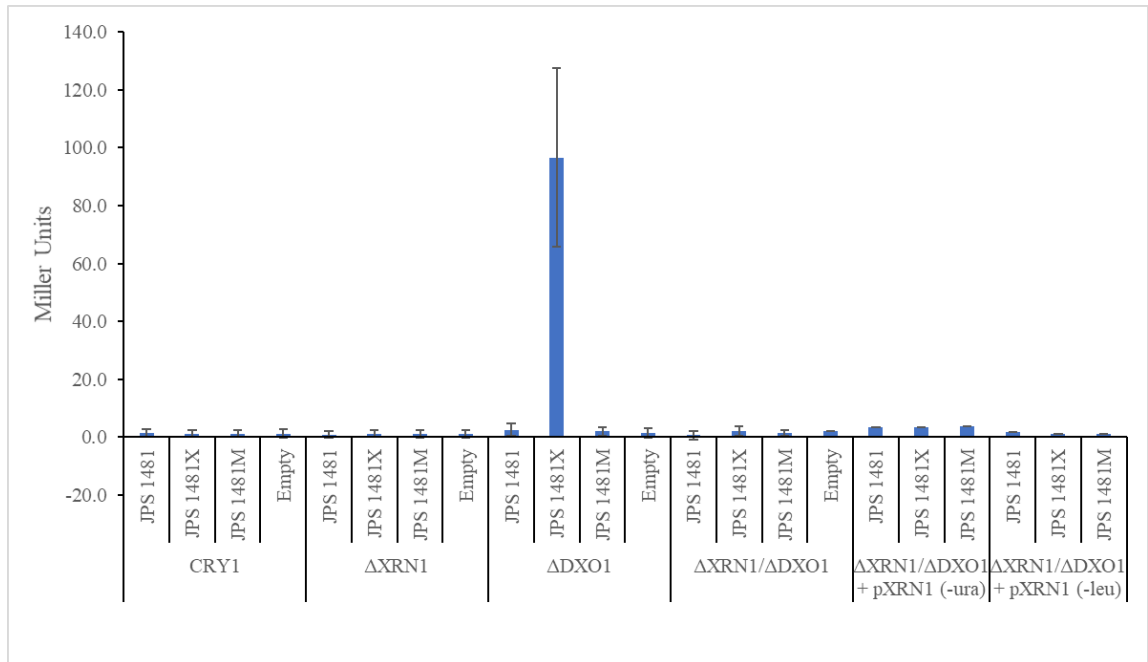
FIGURE S3. β-galactosidase activity of WT CRY1 cells and three different knockout strains expressing three of the reporters from the JPS 1480 series, and the double-knockout strains also expressing two different plasmids containing the *XRN1* ORF. Only the DXO1 knockout appears to have increased enzymatic activity when compared to the empty cells, suggesting that adding the *XRN1* ORF to the double-knockout strain does not genetically rescue IRES activity. The activity of empty cells was also tested to establish a reference point of enzymatic activity.
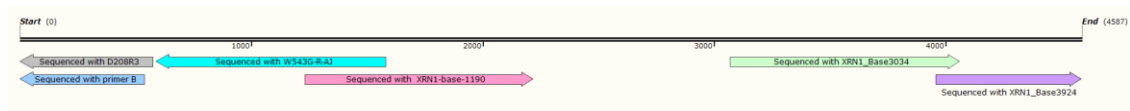
FIGURE S4. Sequencing map of BJH 872 plasmid, encoding pXRN1. Map shows entire length of yeast wild-type *XRN1* gene (black line). Colored arrows indicate fragment that was sequenced using each corresponding primer, as well as direction of the primer.